INTERFERENCE FILTERING

JOHN P. COSTAS

TECHNICAL REPORT NO. 185

MARCH 1, 1951

RESEARCH LABORATORY OF ELECTRONICS
MASSACHUSETTS INSTITUTE OF TECHNOLOGY
CAMBRIDGE, MASSACHUSETTS

The research reported in this document was made possible through support extended the Massachusetts Institute of Technology, Research Laboratory of Electronics, jointly by the Army Signal Corps, the Navy Department (Office of Naval Research) and the Air Force (Air Materiel Command), under Signal Corps Contract No. DA36-039 sc-100, Project No. 8-102B-0; Department of the Army Project No. 3-99-10-022.

MASSACHUSETTS INSTITUTE OF TECHNOLOGY
RESEARCH LABORATORY OF ELECTRONICS

Technical Report No. 185 March 1, 1951

INTERFERENCE FILTERING

John P. Costas

This report is essentially the same as a
doctoral thesis in the Department of Electrical Engineering, M. I. T.

Abstract

The problem of filtering a number of channels of information for the best recovery of one particular channel message is considered in detail. Each channel is assumed to carry a message and a disturbance function, and correlation is assumed to exist between all possible pairs of message and disturbance functions. Exact solutions are obtained for filtering with long delay, and expressions for the irremovable filtering error are derived and discussed.

The synthesis of optimum linear filters by approximation methods is considered. A method of approximation which tends to minimize the filtering error for a given allowable network complexity is given and detailed examples in the use of the method for the general solution of the multiple time series problem are presented.

It is shown that the multichannel filtering techniques may be applied to the problem of detection of amplitude-modulated signals. Adjacent channel interference situations are examined in detail for both double-sideband and single-sideband signals.

Experimental results are presented which verify the theoretical conclusions.

INTERFERENCE FILTERING

I. Statistical Concepts in Communication

A. Transmission of Information

The basic purpose of a communication system is the transmission of information from a transmitter to a receiver. The forms in which communication systems appear are many, but common to all systems is the process of information transmission. The quantity "information" has been defined in different ways (refs. 1, 3, 4). However, certain fundamental conclusions may be drawn concerning information-bearing signals which are consistent with almost any definition of information.

An information-bearing signal or message function can never be considered as a known function of time. Certainly if the future of a message function could be determined exactly from a knowledge of its past, no new information would be received. In short, message functions are necessarily random functions of time and can be described mathematically only in terms of their statistical characteristics.

It becomes quite clear from the foregoing that the design and analysis of communication systems must necessarily utilize the statistical properties of the messages and noises involved.

B. Design of Optimum Linear Systems

The notation used in this report will be exactly that of Lee (ref. 6) and will correspond very closely to that of Wiener (ref. 2). It must be understood that a complete background cannot be given here; only a brief survey of the mathematics is possible. For further discussion the reader is referred to existing literature (refs. 1, 2, 6, 7, 8).

An "optimum" system will be considered one which minimizes the mean-square error between the actual system output $f_o(t)$ and the desired output $f_d(t)$. Thus the mean-square error $\mathcal{E}$ may be written as

$$\mathcal{E} = \lim_{T\to\infty} \frac{1}{2T} \int_{-T}^{T} \left[f_d(t) - f_o(t)\right]^2 dt. \tag{1}$$

If linear systems only are to be considered, the statistical parameters needed for design are known as the correlation functions. The crosscorrelation function $\phi_{12}(\tau)$ between random functions $f_1(t)$ and $f_2(t)$ is defined by

$$\phi_{12}(\tau) = \lim_{T\to\infty} \frac{1}{2T} \int_{-T}^{T} f_1(t) f_2(t+\tau) dt. \tag{2}$$

The autocorrelation function $\phi_{11}(\tau)$ of the random function $f_1(t)$ is defined by

$$\phi_{11}(\tau) = \lim_{T\to\infty} \frac{1}{2T} \int_{-T}^{T} f_1(t) f_1(t+\tau) dt. \tag{3}$$

The Fourier transform pair g(t), G(ω) are related by

$$G(\omega) = \frac{1}{2\pi} \int_{-\infty}^{\infty} g(t)\epsilon^{-j\omega t} dt \tag{4}$$

and

$$g(t) = \int_{-\infty}^{\infty} G(\omega)\epsilon^{+j\omega t} d\omega. \tag{5}$$

By the Laplace transform we shall mean relations (4) and (5) except that ω is replaced by λ where

$$\lambda = \omega + j\sigma. \tag{6}$$

An important theorem due to Wiener (refs. 6, 7) states that the power density spectrum of a random function $f_1(t)$ is given by the Fourier transform of the autocorrelation function of $f_1(t)$. That is

$$\Phi_{11}(\omega) = \frac{1}{2\pi} \int_{-\infty}^{\infty} \phi_{11}(\tau)\epsilon^{-j\omega\tau} d\tau. \tag{7}$$

In a similar manner we may define a cross-power spectrum $\Phi_{12}(\omega)$ between random functions $f_1(t)$ and $f_2(t)$ as

$$\Phi_{12}(\omega) = \frac{1}{2\pi} \int_{-\infty}^{\infty} \phi_{12}(\tau)\epsilon^{-j\omega\tau} d\tau. \tag{8}$$

Let us define the unit impulse u(t) by

$$u(t) = \lim_{a\to\infty} \frac{a}{\sqrt{\pi}} \epsilon^{-a^2t^2}. \tag{9}$$

Then we may show using (4) that the transform U(ω) of u(t) is given by

$$U(\omega) = \frac{1}{2\pi}. \tag{10}$$

Now if h(t) is the response of a linear system to a unit impulse input, it may be shown (ref. 6) that the output $f_o(t)$ of the linear system to an arbitrary input $f_i(t)$ will be given by

$$f_o(t) = \int_{-\infty}^{\infty} h(\sigma) f_i(t-\sigma) d\sigma. \tag{11}$$

Let $e_o(t)$ be the transient output of the linear system due to a transient input $e_i(t)$. If a system function H(ω) is defined for the linear system such that

$$H(\omega) = \frac{E_o(\omega)}{E_i(\omega)} \tag{12}$$

where $E(\omega)$ is the Fourier transform of e(t) it may be shown that $H(\omega)$ and h(t) are related by

$$H(\omega) = \int_{-\infty}^{\infty} h(t)\epsilon^{-j\omega t}dt \tag{13}$$

and

$$h(t) = \frac{1}{2\pi}\int_{-\infty}^{\infty} H(\omega)\epsilon^{+j\omega t}d\omega \tag{14}$$

which correspond to (4) and (5) except for the location of the 2π term.

Since $\Phi_{11}(\omega)$, $\Phi_{12}(\omega)$, and $H(\omega)$ are Fourier transforms of real functions it may be shown from (5) that the real parts of the frequency function are even functions of ω and the imaginary parts odd functions of ω. In particular since it may be shown that

$$\phi_{11}(\tau) = \phi_{11}(-\tau) \tag{15}$$

it follows that $\Phi_{11}(\omega)$ is real. Also since

$$\phi_{12}(\tau) = \phi_{21}(-\tau) \tag{16}$$

it may be shown that

$$\Phi_{12}(\omega) = \Phi_{21}(-\omega). \tag{17}$$

The material in this section is considered of fundamental importance so that use of relations (1) through (17) may be made without specific reference.

II. Optimum Linear Systems for Multiple Time Series

A. General Discussion

Consider the situation described by Fig. 1. Let

$$f_k(t), \quad (1 \leqslant k \leqslant n)$$

represent message functions while

$$g_k(t), \quad (1 \leqslant k \leqslant n)$$

represent disturbance functions. Let it be desired to recover $f_j(t \pm a)$, the j^{th} message predicted or retarded by a seconds. Clearly if there exists no correlation between the j^{th} message or disturbance and any other channel message or disturbance, the only network to be designed will be $H_{jj}(\omega)$ of Fig. 1. The case of single-channel filtering has been treated extensively by Lee (ref. 6) and by Wiener (ref. 2).

If instead we assume that the j^{th} message is correlated to all the other messages

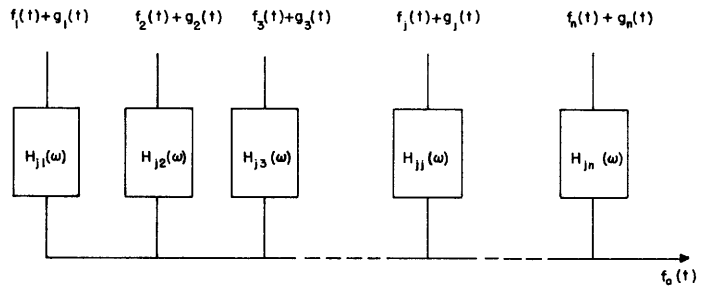

Fig. 1

Multiple time series filtering.

and disturbances as is the j^{th} disturbance, the recovery of $f_j(t\pm a)$ becomes more complex. In this latter case not only must the j^{th} channel be filtered, but so also must every other channel since all other channel voltages are correlated to $f_j(t)$ and $g_j(t)$. By proper treatment of each channel voltage we shall attempt to make the sum of the network outputs give a reinforced j^{th} message and a diminished j^{th} noise. The effect of noise cancellation gives rise to the term "interference" filtering. This writer is indebted to Professor Norbert Wiener for both the basic idea and title of "Interference Filtering".

B. Derivation of the Error Expression

Before continuing it is convenient to define some new symbols. Let the message correlation function $\phi_{jk}^{mm}(\tau)$ be defined by

$$\phi_{jk}^{mm}(\tau) = \lim_{T\to\infty} \frac{1}{2T} \int_{-T}^{T} f_j(t) f_k(t+\tau)\,dt, \tag{18}$$

the disturbance correlation function $\phi_{jk}^{dd}(\tau)$ by

$$\phi_{jk}^{dd}(\tau) = \lim_{T\to\infty} \frac{1}{2T} \int_{-T}^{T} g_j(t) g_k(t+\tau)\,dt, \tag{19}$$

and the message-disturbance crosscorrelation function $\phi_{jk}^{md}(\tau)$ by

$$\phi_{jk}^{md}(\tau) = \lim_{T\to\infty} \frac{1}{2T} \int_{-T}^{T} f_j(t) g_k(t+\tau)\,dt. \tag{20}$$

In addition it is convenient to let

$$\phi_{jk}(\tau) = \phi_{jk}^{mm}(\tau) + \phi_{jk}^{md}(\tau) + \phi_{jk}^{dm}(\tau) + \phi_{jk}^{dd}(\tau) \tag{21}$$

and

$$\psi_{jk}(\tau) = \phi_{jk}^{mm}(\tau) + \phi_{jk}^{dm}(\tau). \tag{22}$$

The output voltage $f_o(t)$ of Fig. 1 is composed of the sum of the individual network

output voltages so that

$$f_o(t) = \sum_{k=1}^{n} \int_{-\infty}^{\infty} d\sigma h_{jk}(\sigma) \left[f_k(t-\sigma) + g_k(t-\sigma) \right]. \tag{23}$$

Now since the desired output is $f_j(t \pm a)$ the mean-square error of the system is

$$\mathcal{E} = \lim_{T \to \infty} \frac{1}{2T} \int_{-T}^{T} dt \left\{ f_j(t \pm a) - \sum_{k=1}^{n} \int_{-\infty}^{\infty} d\sigma h_{jk}(\sigma) \left[f_k(t-\sigma) + g_k(t-\sigma) \right] \right\}^2 \tag{24}$$

which may at once be written as

$$\mathcal{E} = \phi_{jj}^{mm}(o) - 2 \sum_{k=1}^{n} \int_{-\infty}^{\infty} d\sigma h_{jk}(\sigma) \psi_{kj}(\sigma \pm a) + \sum_{k,\, r=1}^{n} \int_{-\infty}^{\infty} \int_{-\infty}^{\infty} d\sigma d\nu h_{jk}(\sigma) h_{jr}(\nu) \phi_{kr}(\sigma - \nu). \tag{25}$$

Equation (25) is the desired error expression. A set of networks $h_{jk}(t)$ must now be found which will make $\mathcal{E}$ minimum.

C. Conditions for Minimum Error

Since $h_{jk}(t)$ is by definition the response of the k^{th} network to a unit impulse input, it must be kept in mind that

$$h_{jk}(t) = 0 \quad \text{for all} \quad t < 0. \tag{26}$$

Any solution which makes $\mathcal{E}$ of (25) a minimum must also satisfy (26) if the solution is to be physically realizable.

Let $h_{jk}(t)$ take on an admissible variation $\epsilon_k \eta_k(t)$ where ϵ_k is a parameter independent of $\eta_k(t)$ and $h_{jk}(t)$. By an admissible variation it is meant that

$$\eta_k(t) = 0 \quad \text{for} \quad t < 0. \tag{27}$$

Thus if $h_{jk}(t)$ is replaced by $h_{jk}(t) + \epsilon_k \eta_k(t)$ in (25) $\mathcal{E}$ will also take on a variation $\delta \mathcal{E}$ so that

$$\mathcal{E} + \delta\mathcal{E} = \phi_{jj}^{mm}(o) - 2 \sum_{k=1}^{n} \int_{-\infty}^{\infty} d\sigma \left[h_{jk}(\sigma) + \epsilon_k \eta_k(\sigma) \right] \psi_{kj}(\sigma \pm a) + \sum_{k,\, r=1}^{n} \int_{-\infty}^{\infty} \int_{-\infty}^{\infty} d\sigma d\nu$$

$$\left[h_{jk}(\sigma) + \epsilon_k \eta_k(\sigma) \right] \left[h_{jr}(\nu) + \epsilon_r \eta_r(\nu) \right] \phi_{kr}(\sigma - \nu). \tag{28}$$

Now if a set of networks $h_{jk}(t)$ is chosen such that $\mathcal{E}$ of (25) is a minimum then from (28) we must have

$$\left. \frac{\partial \left[\mathcal{E} + \delta \mathcal{E} \right]}{\partial \epsilon_q} \right|_{\epsilon_1, \epsilon_2, \epsilon_3 \cdots \epsilon_n = 0} = 0, \qquad (1 \leq q \leq n). \tag{29}$$

Furthermore (29) must hold for any admissible set of variations $\eta_q(t)$. The set of networks $h_{jk}(t)$ which makes $\mathcal{E}$ minimum must necessarily satisfy (29). Thus

$$\left.\frac{\partial[\mathcal{E}+\delta\mathcal{E}]}{\partial\epsilon_q}\right|_{\epsilon_1=\cdots=\epsilon_n=0} = -2\int_{-\infty}^{\infty} d\sigma\eta_q(\sigma)\psi_{qj}(\sigma\pm a) + 2\sum_{k=1}^{n}\int_{-\infty}^{\infty}\int_{-\infty}^{\infty} d\sigma d\nu\phi_{kq}(\nu-\sigma)h_{jk}(\nu)\eta_q(\sigma) = 0 \qquad (30)$$

$$(1\leqslant q\leqslant n)$$

which may be rewritten as

$$\int_{-\infty}^{\infty} d\sigma\eta_q(\sigma)\left\{\sum_{k=1}^{n}\int_{-\infty}^{\infty} d\nu\phi_{kq}(\nu-\sigma)h_{jk}(\nu) - \psi_{qj}(\sigma\pm a)\right\} = 0 \qquad (31)$$

$$(1\leqslant q\leqslant n).$$

Since the above relation must hold for any admissible $\eta_q(\sigma)$ we may write at once that

$$\sum_{k=1}^{n}\int_{-\infty}^{\infty} d\nu\phi_{kq}(\nu-\sigma)h_{jk}(\nu) = \psi_{qj}(\sigma\pm a) \qquad (32)$$

$$\text{for } \sigma>0 \qquad (1\leqslant q\leqslant n).$$

Any set of networks $h_{jk}(t)$ which makes $\mathcal{E}$ of (25) a minimum must also satisfy (32). It must now be shown that solutions of (32) are networks giving minimum $\mathcal{E}$ and not maximum or stationary solutions.

In order to prove that solutions of (32) always result in minimum $\mathcal{E}$ we shall show that $\delta\mathcal{E}$ of (28) is always positive if (32) is satisfied.

From (28) we have

$$\delta\mathcal{E} = 2\sum_{k,\,r=1}^{n}\int_{-\infty}^{\infty}\int_{-\infty}^{\infty} d\sigma d\nu\phi_{kr}(\sigma-\nu)\epsilon_k\eta_k(\sigma)\left[h_{jr}(\nu)+\epsilon_r\eta_r(\nu)\right] - 2\sum_{k=1}^{n}\int_{-\infty}^{\infty} d\sigma\psi_{kj}(\sigma\pm a)\epsilon_k\eta_k(\sigma). \qquad (33)$$

In (32) change k to r, q to k and obtain

$$\sum_{r=1}^{n}\int_{-\infty}^{\infty} d\nu\phi_{rk}(\nu-\sigma)h_{jr}(\nu) = \psi_{kj}(\sigma\pm a) \qquad (34)$$

$$\text{for } \sigma>0 \qquad (1\leqslant k\leqslant n).$$

Now multiplying both sides of (34) by $\epsilon_k \eta_k(\sigma)d\sigma$ and integrating from $-\infty$ to ∞ in σ and at the same time summing over k from 1 to n we get

$$\sum_{k,\,r=1}^{n} \int_{-\infty}^{\infty} \int_{-\infty}^{\infty} d\sigma d\nu \phi_{kr}(\sigma-\nu) h_{jr}(\nu) \epsilon_k \eta_k(\sigma) = \sum_{k=1}^{n} \int_{-\infty}^{\infty} d\sigma \psi_{kj}(\sigma \pm a) \epsilon_k \eta_k(\sigma). \tag{35}$$

When (35) is substituted into (33) there results

$$\delta \mathcal{E} = 2 \sum_{k,\,r=1}^{n} \epsilon_k \epsilon_r \int_{-\infty}^{\infty} \int_{-\infty}^{\infty} d\sigma d\nu \phi_{kr}(\sigma-\nu) \eta_k(\sigma) \eta_r(\nu). \tag{36}$$

Note that in trying to prove $\delta\mathcal{E}$ always positive it must be realized that the ϵ_k are arbitrary as are the $\eta_k(\sigma)$ provided (27) is satisfied.

Since the η_k satisfy (27), physical networks may be built having $\eta_k(t)$ as impulse responses. Let the k^{th} channel voltage $e_k(t)$ where

$$e_k(t) = f_k(t) + g_k(t) \tag{37}$$

be the input to the $\eta_k(t)$ network and let $e'_k(t)$ be the output as shown in Fig. 2. Now the crosscorrelation $\phi'_{kr}(\tau)$ between $e'_k(t)$ and $e'_r(t)$ is

$$\phi'_{kr}(\tau) = \int_{-\infty}^{\infty} \int_{-\infty}^{\infty} d\sigma d\nu \eta_k(\sigma) \eta_r(\nu) \phi_{kr}(\tau+\sigma-\nu) \tag{38}$$

where

$$\phi'_{kr}(\tau) = \lim_{T\to\infty} \frac{1}{2T} \int_{-T}^{T} e'_k(t) e'_r(t+\tau) dt. \tag{39}$$

The double integral expression of (36) is given by (38) if τ is set equal to zero. Thus (36) becomes

$$\delta \mathcal{E} = 2 \sum_{k,\,r=1}^{n} \epsilon_k \epsilon_r \phi'_{kr}(0). \tag{40}$$

Since the ϵ_k and η_k are all real valued we have the following inequality

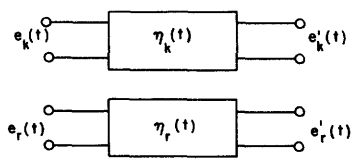

Fig. 2
Variational network pair.

$$\left[\sum_{k=1}^{n} \epsilon_k e'_k(t)\right]^2 \geq 0 \tag{41}$$

which may be written as

$$\sum_{k,\,r=1}^{n} \epsilon_k \epsilon_r e_k'(t) e_r'(t) \geq 0. \tag{42}$$

If the time average is taken of both sides of (42) one obtains

$$\sum_{k,\,r=1}^{n} \epsilon_k \epsilon_r \phi_{kr}'(0) \geq 0 \tag{43}$$

which means that $\delta\mathcal{E} \geq 0$ for all ϵ_k and all admissible η_k. Since the equality in (43) holds only in the trivial case where all channel voltages are zero one can be sure that solutions of (32) will yield a minimum system mean-square error.

To obtain expressions for the minimum error multiply both sides of (34) by $h_{jk}(\sigma)d\sigma$ and integrate from $-\infty$ to ∞ in σ. At the same time sum over k from 1 to n getting

$$\sum_{k,\,r=1}^{n} \int_{-\infty}^{\infty} \int_{-\infty}^{\infty} d\sigma\, d\nu\, \phi_{kr}(\sigma-\nu) h_{jr}(\nu) h_{jk}(\sigma) = \sum_{k=1}^{n} \int_{-\infty}^{\infty} d\sigma \psi_{kj}(\sigma \pm a) h_{jk}(\sigma). \tag{44}$$

The above expression when substituted into (25) gives the minimum error, $\mathcal{E}_{min}$, where

$$\mathcal{E}_{min} = \phi_{jj}^{mm}(0) - \sum_{k=1}^{n} \int_{-\infty}^{\infty} d\sigma\, h_{jk}(\sigma) \psi_{kj}(\sigma \pm a) \tag{45}$$

or in terms of Fourier transforms

$$\mathcal{E}_{min} = \int_{-\infty}^{\infty} d\omega \left\{ \Phi_{jj}^{mm}(\omega) - \sum_{k=1}^{n} \Psi_{kj}(\omega) H_{jk}(-\omega) \epsilon^{\pm j\omega a} \right\}. \tag{46}$$

It must be remembered that the network functions which appear in (45) and (46) are not arbitrary but are solutions of (32).

D. Network Solutions for Long Delay Filtering

The general solution of the set of equations (32) is left to the approximation method of Sec. III. For an exact general solution the reader is referred to Wiener's method of undetermined coefficients (ref. 2). Since the best possible recovery of the j^{th} message will be obtained if a long delay is allowed in the system (ref. 6), the long delay solution will give indications as to the ultimate filtering possibilities for given input messages and noises. It must be kept in mind that "long" is used in a comparative sense here. For example, one-tenth of one second may be considered a long time where speech voltages are concerned.

First let (32) be rewritten as

$$\sum_{k=1}^{n} \int_{-\infty}^{\infty} d\nu \phi_{qk}(\sigma - \nu) h_{jk}(\nu) - \psi_{qj}(\sigma \pm a) = P_q(\sigma) \qquad (1 \leq q \leq n). \tag{47}$$

where $p_q(\sigma)$ is a function having the property

$$p_q(\sigma) = 0 \quad \text{for} \quad \sigma > 0. \tag{48}$$

Taking the Laplace transform of both sides of (47) we obtain

$$\sum_{k=1}^{n} \Phi_{qk}(\lambda) H_{jk}(\lambda) - \Psi_{qj}(\lambda) \epsilon^{\pm j a \lambda} = P_q(\lambda) \qquad (1 \leq q \leq n). \tag{49}$$

Let $\Phi_{qq}(\lambda)$ be factorable so that

$$\Phi_{qq}(\lambda) = \Phi^{+}_{qq}(\lambda) \Phi^{-}_{qq}(\lambda) \tag{50}$$

where $\Phi^{+}_{qq}(\lambda)$ has all its poles and zeros in the upper half of the λ plane and $\Phi^{-}_{qq}(\lambda)$ has all its poles and zeros in the lower half of the λ plane. Poles or zeros will not occur on the ω axis of the λ plane as $\Phi_{qq}(\omega)$ is the power density spectrum of a random time function.

Then (49) may be written as

$$H_{jq}(\lambda) \Phi^{+}_{qq}(\lambda) + \sum_{k=1}^{n}{}' \frac{\Phi_{qk}(\lambda) H_{jk}(\lambda)}{\Phi^{-}_{qq}(\lambda)} - \frac{\Psi_{qj}(\lambda) \epsilon^{\pm j a \lambda}}{\Phi^{-}_{qq}(\lambda)} = \frac{P_q(\lambda)}{\Phi^{-}_{qq}(\lambda)} \qquad (1 \leq q \leq n). \tag{51}$$

where the prime after the summation sign indicates that the k=q term is missing. Let

$$R(\lambda) = \sum_{k=1}^{n}{}' \frac{\Phi_{qk}(\lambda)}{\Phi^{-}_{qq}(\lambda)} H_{jk}(\lambda) - \frac{\Psi_{qj}(\lambda) \epsilon^{\pm j a \lambda}}{\Phi^{-}_{qq}(\lambda)}. \tag{52}$$

Then (51) may be written as

$$H_{jq}(\lambda) \Phi^{+}_{qq}(\lambda) + \frac{1}{2\pi} \int_{0}^{\infty} \epsilon^{-j\lambda t} dt \int_{-\infty}^{\infty} R(\omega) \epsilon^{+j\omega t} d\omega$$

$$+ \frac{1}{2\pi} \int_{-\infty}^{0} \epsilon^{-j\lambda t} dt \int_{-\infty}^{\infty} R(\omega) \epsilon^{+j\omega t} d\omega = \frac{P_q(\lambda)}{\Phi^{-}_{qq}(\lambda)}. \tag{53}$$

Now the first two terms on the left have all their poles, if any, in the upper half of the

λ plane. The last term on the left and the term on the right have all their poles in the lower half of the λ plane. Thus the first two terms on the left must sum equal to a constant since they cannot have poles in either half of the λ plane. Therefore

$$H_{jq}(\lambda)\Phi^{+}_{qq}(\lambda) + \frac{1}{2\pi}\int_{0}^{\infty} \epsilon^{-j\lambda t}dt \int_{-\infty}^{\infty} R(\omega)\epsilon^{+j\omega t}d\omega = \text{constant} \qquad (54)$$

$$(1 \leqslant q \leqslant n).$$

It can be shown that the constant term of this equation must be chosen as zero so that

$$H_{jq}(\lambda) = \frac{1}{2\pi\Phi^{+}_{qq}(\lambda)} \int_{0}^{\infty} \epsilon^{-j\lambda t}dt \int_{-\infty}^{\infty} \frac{\Psi_{qj}(\omega)\epsilon^{\pm ja\omega} - \sum_{k=1}^{n}{}' \Phi_{qk}(\omega)H_{jk}(\omega)}{\Phi^{-}_{qq}(\omega)} \epsilon^{j\omega t}d\omega \qquad (55)$$

$$(1 \leqslant q \leqslant n).$$

This last equation yields a general solution only for $n=1$. For $\eta > 1$ the system function of the q^{th} network is expressed in terms of all the other network system functions in the rather complex form of (55).

For long delay filtering it is convenient to define

$$H_{jk}(\lambda) = H'_{jk}(\lambda)\epsilon^{-ja\lambda} \qquad (56)$$

and rewrite (55) as

$$H_{jq}(\lambda) = \frac{1}{2\pi\Phi^{+}_{qq}(\lambda)} \int_{0}^{\infty} dt\epsilon^{-j\lambda t}$$

$$\int_{-\infty}^{\infty} \frac{\Psi_{qj}(\omega)\epsilon^{-ja\omega} - \sum_{k=1}^{n}{}' \Phi_{qk}(\omega)H'_{jk}(\omega)\epsilon^{-ja\omega}}{\Phi^{-}_{qq}(\omega)} \epsilon^{j\omega t}d\omega \qquad (57)$$

$$(1 \leqslant q \leqslant n).$$

As $a \to \infty$ the lower limit of zero in the time integration of (57) may be changed to $-\infty$ and we have

$$H_{jq}(\lambda) = \frac{\Psi_{qj}(\lambda) - \sum_{k=1}^{n}{}' \Phi_{qk}(\lambda)H'_{jk}(\lambda)}{\Phi_{qq}(\lambda)} \epsilon^{-ja\lambda} \qquad (58)$$

for $a \to \infty$ $\qquad (1 \leqslant q \leqslant n)$

or

$$\sum_{k=1}^{n} H'_{jk}(\lambda)\Phi_{qk}(\lambda) = \Psi_{qj}(\lambda)$$
$$\text{for } a \to \infty \qquad (1 \leq q \leq n). \tag{59}$$

The set of equations (59) may now be solved quite easily for $H'_{jq}(\lambda)$, that is

$$H'_{jq}(\lambda) = \frac{\begin{vmatrix} \Phi_{11}(\lambda) & \cdots & \Psi_{1j}(\lambda) & \cdots & \Phi_{1n}(\lambda) \\ \Phi_{21}(\lambda) & \cdots & \Psi_{2j}(\lambda) & \cdots & \Phi_{2n}(\lambda) \\ \vdots & & \vdots & & \vdots \\ \Phi_{n1}(\lambda) & \cdots & \Psi_{nj}(\lambda) & \cdots & \Phi_{nn}(\lambda) \end{vmatrix}}{\begin{vmatrix} \Phi_{11}(\lambda) & \Phi_{12}(\lambda) & \cdots & \Phi_{1n}(\lambda) \\ \Phi_{21}(\lambda) & \Phi_{22}(\lambda) & \cdots & \Phi_{2n}(\lambda) \\ \vdots & \vdots & & \vdots \\ \Phi_{n1}(\lambda) & \Phi_{n2}(\lambda) & \cdots & \Phi_{nn}(\lambda) \end{vmatrix}} \tag{60}$$

In particular for j=1, n=1

$$H'_{11}(\lambda) = \frac{\Psi_{11}(\lambda)}{\Phi_{11}(\lambda)} \tag{61}$$

and for j=1, n=2

$$H'_{11}(\lambda) = \frac{\Psi_{11}(\lambda)\Phi_{22}(\lambda) - \Psi_{21}(\lambda)\Phi_{12}(\lambda)}{\Phi_{11}(\lambda)\Phi_{22}(\lambda) - \Phi_{21}(\lambda)\Phi_{12}(\lambda)} \tag{62}$$

and

$$H'_{12}(\lambda) = \frac{\Psi_{21}(\lambda)\Phi_{11}(\lambda) - \Psi_{11}(\lambda)\Phi_{21}(\lambda)}{\Phi_{11}(\lambda)\Phi_{22}(\lambda) - \Phi_{21}(\lambda)\Phi_{12}(\lambda)}\,. \tag{63}$$

E. Irremovable Error Considerations

Since the best possible filtering is obtained in the long delay case, an expression for the irremovable error $\mathcal{E}_{irr}$ may be derived by using the long delay network solutions of (60) in the minimum error expression of (46). From (56) and (46) we see that

$$\mathcal{E}_{irr} = \int_{-\infty}^{\infty} d\omega \left\{ \Phi_{jj}^{mm}(\omega) - \sum_{k=1}^{n} \Psi_{kj}(\omega) H'_{jk}(-\omega) \right\}. \tag{64}$$

For the special case j=1, n=1 using (61) we have

$$\mathcal{E}_{irr} = \int_{-\infty}^{\infty} \frac{\Phi_{11}^{mm}(\omega)\Phi_{11}(\omega) - |\Psi_{11}(\omega)|^2}{\Phi_{11}(\omega)}\, d\omega \tag{65}$$

which is in agreement with the expression given by Lee (ref. 6). If in addition the message $f_1(t)$ is not correlated to the disturbance $g_1(t)$, (65) becomes

$$\mathcal{E}_{irr} = \int_{-\infty}^{\infty} \frac{\Phi_{11}^{mm}(\omega)\ \Phi_{11}^{dd}(\omega)}{\Phi_{11}^{mm}(\omega) + \Phi_{11}^{dd}(\omega)}\, d\omega. \tag{66}$$

For the case j=1, n=2 (64) becomes

$$\mathcal{E}_{irr} = \int_{-\infty}^{\infty} d\omega \left\{\Phi_{11}^{mm}(\omega) - \Psi_{11}(\omega)H_{11}'(-\omega) - \Psi_{21}(\omega)H_{12}'(-\omega)\right\} \tag{67}$$

where $H_{11}'(-\omega)$ and $H_{12}'(-\omega)$ may be derived from (62) and (63) respectively. These special cases will be investigated in greater detail in Sec. IV.

III. An Approximation Method for the General Treatment of Multiple Time Series

A. Conventional Approximation Technique

Let us consider for the moment the filtering of a single time series. Setting n=1 in (55) there results

$$H_{11}(\lambda) = \frac{1}{2\pi\Phi_{11}^{+}(\lambda)} \int_0^{\infty} dt\epsilon^{-j\lambda t} \int_{-\infty}^{\infty} \frac{\Psi_{11}(\omega)\epsilon^{\pm j a\omega}}{\Phi_{11}^{-}(\omega)}\, \epsilon^{+j\omega t} d\omega \tag{68}$$

which is the well-known optimum filter formula (refs. 2, 6). Thus, if the correlation functions of the message and noise are known, (68) will give the ideal system function $H_{11}(\lambda)$ from which the ideal impulse response $h_{11}(t)$ may be obtained. Since in general $H_{11}(\lambda)$ will not be a rational function of λ, some type of approximation method must be used for actual network realization.

Let the ideal impulse response $h_{11}(t)$ be represented by an infinite series of orthonormal functions $u_s(t)$, that is

$$h_{11}(t) = \sum_{s=1}^{\infty} c_s u_s(t). \tag{69}$$

The set of functions $u_s(t)$ has the property that (refs. 9, 10)

$$\int_0^{\infty} u_r(t)u_s(t)dt = \begin{cases} 0, & r \neq s \\ 1, & r = s \end{cases} \tag{70}$$

so that the coefficient of the expansion may be determined from

$$c_s = \int_0^{\infty} u_s(t)h_{11}(t)dt. \tag{71}$$

We must limit ourselves, of course, to those orthonormal sets $u_s(t)$ having transforms $U_s(\omega)$ which are rational functions of frequency (refs. 2, 6, 9, 10).

Practical considerations limit the degree of the approximation; that is, the network to be built will have an impulse response $h_{11}^{app}(t)$ where

$$h_{11}^{app}(t) = \sum_{s=1}^{N} c_s u_s(t). \tag{72}$$

The impulse response (72) is the series (69) terminated with the N^{th} term. The approximate system function $H_{11}^{app}(\omega)$, where

$$H_{11}^{app}(\omega) = \sum_{s=1}^{N} c_s U_s(\omega) \tag{73}$$

is a rational function of ω and a network may be built having (73) as its transfer function (refs. 11, 13).

The method outlined above has been used with success, but certain disadvantages are to be noted. First, the terminated series (72) has the property that the coefficients c_s as given by (71) will yield the least integral of the squared error between the ideal and approximate impulse response (refs. 9, 10). That is

$$\int_0^\infty \left[h_{11}^{app}(t) - h_{11}(t)\right]^2 dt \tag{74}$$

is minimized by this method. However, it is not (74) that we wish to minimize with a given complexity of network, but the filtering error $\mathcal{E}$, where

$$\mathcal{E} = \lim_{T\to\infty} \frac{1}{2T} \int_{-T}^{T} \left[f_o(t) - f_1(t\pm a)\right]^2 dt. \tag{75}$$

Lee has clearly shown (ref. 6) that the condition of minimum approximation error (74) is quite different, in general, from the condition of minimum filtering error (75). In short, the conventional method is aimed at getting the best approximation of an ideal response for a given network complexity rather than getting the best possible filtering.

The amount of work required is generally large; however, several ingenious techniques have been devised to expedite the synthesis (ref. 14).

B. An Improved Method of Network Realization

It is quite clear that since, in general, the ideal transfer function $H_{11}(\omega)$ is not a rational frequency function, a perfect job of network synthesis can never be done. How closely this ideal may be approached depends on the allowable complexity of the network. Since practical considerations limit the number of elements in a given filter we must

content ourselves with something less than a perfect job. Within the constraints imposed by practical or engineering considerations we must design for the best possible filtering performance. An example of such an approach is given in the following section.

C. Derivation of Design Equations

Returning to the multiple time series problem of Fig. 1 let the networks $H_{jk}(\omega)$ be limited to RC networks. Furthermore, let the poles of $H_{jk}(\omega)$ be at $\lambda = jp,\ j2p, j3p, ---,$ jNp. Thus the impulse response $h_{jk}(t)$ must be of the form

$$\left.\begin{aligned} h_{jk}(t) &= \sum_{s=1}^{N} c_s^{jk}\, \epsilon^{-spt} \qquad \text{for } t>0 \\ \text{and} \\ h_{jk}(t) &= 0 \qquad\qquad\qquad \text{for } t<0. \end{aligned}\right\} \tag{76}$$

Sets of coefficients c_s^{jk} must now be found to make $\mathcal{E}$ of (25) a minimum. Substituting (76) into (25) gives

$$\begin{aligned} \mathcal{E} = \phi_{jj}^{mm}(0) &- 2 \sum_{k,\,s=1}^{n,\,N} c_s^{jk} \int_0^\infty d\sigma\, \epsilon^{-sp\sigma} \psi_{kj}(\sigma \pm a) \\ &+ \sum_{k,\,r,\,s,\,u=1}^{n,\,n,\,N,\,N} c_s^{jk} c_u^{jr} \int_0^\infty \int_0^\infty d\sigma\, d\nu\, \epsilon^{-sp\sigma}\, \epsilon^{-up\nu}\, \phi_{kr}(\sigma-\nu). \end{aligned} \tag{77}$$

Now a necessary condition for making $\mathcal{E}$ a minimum is that

$$\frac{\partial \mathcal{E}}{\partial c_m^{jq}} = 0 \qquad \text{for all } (1 \leqslant q \leqslant n) \text{ and } (1 \leqslant m \leqslant N). \tag{78}$$

Performing the differentiation one obtains

$$\sum_{u,\,r=1}^{N,\,n} c_u^{jr} \int_0^\infty \int_0^\infty d\sigma\, d\nu\, \phi_{qr}(\sigma-\nu)\, \epsilon^{-mp\sigma}\, \epsilon^{-up\nu} = \int_0^\infty d\sigma\, \psi_{qj}(\sigma \pm a)\, \epsilon^{-mp\sigma} \tag{79}$$

for all $(1 \leqslant q \leqslant n)$ and $(1 \leqslant m \leqslant N)$.

For convenience, changing m to s and q to k results in

$$\sum_{u,\,r=1}^{N,\,n} c_u^{jr} \int_0^\infty \int_0^\infty d\sigma\, d\nu\, \phi_{kr}(\sigma-\nu)\, \epsilon^{-sp\sigma}\, \epsilon^{-up\nu} = \int_0^\infty d\sigma\, \psi_{kj}(\sigma \pm a)\, \epsilon^{-sp\sigma} \tag{80}$$

for all $(1 \leqslant k \leqslant n)$ and $(1 \leqslant s \leqslant N)$.

Thus (80) represents $n \times N$ equations in the $n \times N$ c_u^{jr} unknowns.

It must now be shown that solutions of (80) represent minimum error conditions.

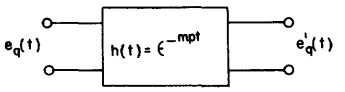

Fig. 3
Network for minimization proof.

Taking the second partial derivative of $\mathcal{E}$ with respect to c_m^{jq} we get from (77)

$$\frac{\partial^2 \mathcal{E}}{\partial c_m^{jq2}} = 2 \int_0^\infty \int_0^\infty d\sigma d\nu \, \phi_{qq}(\sigma-\nu)\epsilon^{-mp(\sigma+\nu)} \qquad (81)$$

$(1 \leq m \leq N), \quad (1 \leq q \leq n).$

Consider now the situation of Fig. 3. The input voltage $e_q(t)$ is the q^{th} channel message plus noise voltage. The output voltage $e'_q(t)$ has an autocorrelation function $\phi'_{qq}(\tau)$ which may be shown to be given by

$$\phi'_{qq}(\tau) = \int_0^\infty \int_0^\infty d\sigma d\nu \, \epsilon^{-mp(\sigma+\nu)} \phi_{qq}(\tau+\sigma-\nu). \qquad (82)$$

Thus (81) may be written as

$$\frac{\partial^2 \mathcal{E}}{\partial c_m^{jq2}} = 2\phi'_{mm}(0) \geq 0. \qquad (83)$$

The equality holds only for the trivial case when the q^{th} channel voltage is zero, so that solutions of (80) will yield minimum filtering error.

It is now important to find the mean-square error which results if (80) is satisfied. Multiplying both sides of (80) by c_s^{jk} and summing over k and s from 1 to n and 1 to N respectively we find

$$\sum_{k,r,s,u=1}^{n,n,N,N,} c_s^{jk} c_u^{jr} \int_0^\infty \int_0^\infty d\sigma d\nu \phi_{kr}(\sigma-\nu)\epsilon^{-sp\sigma}\epsilon^{-up\nu} = \sum_{k,s=1}^{n,N} c_s^{jk} \int_0^\infty d\sigma \psi_{kj}(\sigma \pm a)\epsilon^{-sp\sigma}. \qquad (84)$$

When (84) is substituted into (77) one obtains for the minimum filtering error

$$\mathcal{E}_{min} = \phi_{jj}^{mm}(0) - \sum_{k,s=1}^{n,N} c_s^{jk} \int_0^\infty d\sigma \epsilon^{-sp\sigma} \psi_{kj}(\sigma \pm a). \qquad (85)$$

Note that the integral involved in (85) is also found in (79) so that $\mathcal{E}_{min}$ may be obtained quite easily once a solution of (80) is made.

Consider now the special case of j=1, n=1. From (80) we have

$$\sum_{u=1}^{N} c_u^{11} \int_0^\infty \int_0^\infty d\sigma d\nu \phi_{11}(\sigma-\nu)\epsilon^{-sp\sigma}\epsilon^{-up\nu} = \int_0^\infty d\sigma \psi_{11}(\sigma \pm a)\epsilon^{-sp\sigma} \qquad (86)$$

for $(1 \leq s \leq N)$

and from (85)

$$\mathcal{E}_{min} = \phi_{11}^{mm}(0) - \sum_{s=1}^{N} c_s^{11} \int_0^\infty d\sigma\, \epsilon^{-sp\sigma} \psi_{11}(\sigma \pm a). \tag{87}$$

For j=1, n=2 we have

$$\sum_{u=1}^{N} c_u^{11} \int_0^\infty \int_0^\infty d\sigma d\nu \phi_{k1}(\sigma-\nu) \epsilon^{-sp\sigma} \epsilon^{-up\nu} + \sum_{u=1}^{N} c_u^{12} \int_0^\infty \int_0^\infty d\sigma d\nu \phi_{k2}(\sigma-\nu) \epsilon^{-sp\sigma} \epsilon^{-up\nu}$$

$$= \int_0^\infty d\sigma \psi_{k1}(\sigma \pm a) \epsilon^{-sp\sigma} \tag{88}$$

$$\text{for } k = 1, 2 \text{ and } (1 \leqslant s \leqslant N)$$

and for $\mathcal{E}_{min}$

$$\mathcal{E}_{min} = \phi_{11}^{mm}(0) - \sum_{s=1}^{N} c_s^{11} \int_0^\infty d\sigma\, \epsilon^{-sp\sigma} \psi_{11}(\sigma \pm a)$$

$$- \sum_{s=1}^{N} c_s^{12} \int_0^\infty d\sigma\, \epsilon^{-sp\sigma} \psi_{21}(\sigma \pm a). \tag{89}$$

Detailed examples of these special cases may be found in Sec. V.

D. Realization of Networks

From the work of the previous section it can be seen that the network transfer functions will be of the form

$$H_{jk}(\lambda) = \sum_{s=1}^{N} \frac{c_s^{jk}}{j\lambda + sp}. \tag{90}$$

The poles of this transfer function all lie on the σ axis in the upper half of the λ plane. The residues at these poles are all real so that (90) can always be synthesized as an RC network (refs. 11, 12, 13). With little difficulty a symmetrical RC lattice may be designed (ref. 13) and Guillemin has shown (ref. 15) that (90) may always be realized as an unbalanced structure composed of paralleled RC ladders. If active networks are considered the synthesis becomes considerably simplified.

The transfer function (90) cannot be realized as a driving-point impedance since, in general, some of the c_s^{jk} terms will be negative. However, if (90) is written in the form

$$H_{jk}(\lambda) = \left[\sum_{s \text{ for } +c_s^{jk}} \frac{(+c_s^{jk})}{j\lambda + sp} \right] - \left[\sum_{s \text{ for } -c_s^{jk}} \frac{(-c_s^{jk})}{j\lambda + sp} \right] \tag{91}$$

both bracketed terms may be realized as RC driving point impedances. Since $H_{jk}(\lambda)$ is equal to the difference between two impedances, that is

$$H_{jk}(\lambda) = Z_1(\lambda) - Z_2(\lambda) \tag{92}$$

we may realize this transfer function by the method shown in Fig. 4. An electronic filter of the form of Fig. 4 has been designed and operated successfully. A detailed description of this work may be found in Sec. V. Thus through the use of active elements the design of the filter is reduced simply to the synthesis of RC impedances Z_1 and Z_2.

IV. Application of Interference Filtering Theory to the Detection of Amplitude-Modulated Signals

A. Synchronous Detection of Amplitude-Modulated Signals

If a message function $f_m(t)$ amplitude modulates a carrier wave of frequency ω_o the resultant amplitude-modulated signal $f_s(t)$ may be written

$$f_s(t) = \left[A_o + f_m(t)\right]\cos \omega_o t. \tag{93}$$

Since it will later be shown that the carrier component is basically unimportant (93) may be written

$$f_s(t) = f_m(t)\cos \omega_o t \tag{94}$$

and by an a-m signal we shall mean a signal of the form (94). The process of amplitude modulation is, therefore, essentially one of multiplication in the time domain. To determine the significance of the process in the frequency domain we first find the autocorrelation function $\phi_{ss}(\tau)$ of the a-m signal which is given by

$$\phi_{ss}(\tau) = \frac{\phi_{mm}(\tau)}{2} \cos \omega_o \tau \tag{95}$$

which when transformed yields

$$\Phi_{ss}(\omega) = \frac{1}{4}\left[\Phi_{mm}(\omega - \omega_o) + \Phi_{mm}(\omega + \omega_o)\right]. \tag{96}$$

Thus, in the frequency domain the modulation process results in a shift of the message

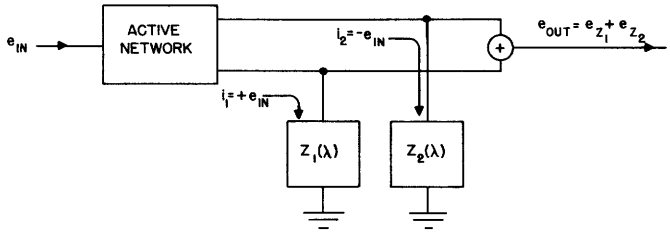

Fig. 4
A possible scheme for network realization.

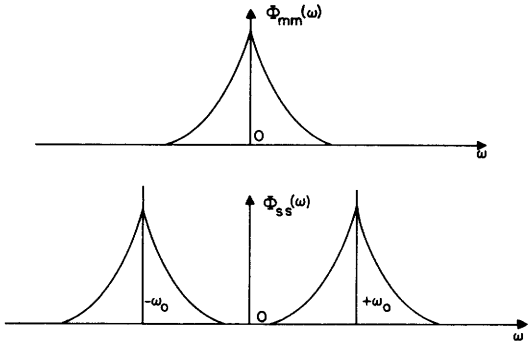

Fig. 5

(top) Original message spectrum.
(bottom) Resultant a-m signal spectrum.

spectrum by an amount ω_o. This situation is described by Fig. 5.

Since the process of amplitude modulation is essentially one of spectrum shift, a possible detection method immediately presents itself. That is, detect the a-m signal by shifting the message spectrum back to its original position about $\omega = 0$. Thus in the time domain such a detection process would appear as

$$f_s(t) \cos \omega_o t = \frac{f_m(t)}{2} \left[1 + \cos 2\omega_o t\right] \quad (97)$$

which when put through a low-pass filter will give

$$f_s(t) \cos \omega_o t\Big]_{L.P.} = \frac{f_m(t)}{2}. \quad (98)$$

This method is by no means new (refs. 16, 17, 18).

One advantage of synchronous detection that has attracted much attention is the possibility of "phase duplexing" two messages in a given a-m channel. Let $f_1(t)$ and $f_2(t)$ be two messages which amplitude modulate cosine and sine carriers respectively at a frequency ω_o. The transmitted signal, $f_s(t)$, would then be given by

$$f_s(t) = f_1(t) \cos \omega_o t + f_2(t) \sin \omega_o t. \quad (99)$$

Now at the receiver, voltages $\cos \omega_o t$ and $\sin \omega_o t$ are generated and the low frequency components of the following products are taken

$$f_s(t) \cos \omega_o t\Big]_{L.P.} = \frac{f_1(t)}{2} \quad (100)$$

and

$$f_s(t) \sin \omega_o t\Big]_{L.P.} = \frac{f_2(t)}{2}. \quad (101)$$

Thus, the two messages may be detected separately at the receiver. In this way the bandwidth conservation properties of single sideband transmission may be realized with a possible reduction in the complexity of terminal equipment.

This "two-phase" method of detection may prove useful even though a single message is being transmitted in the a-m channel. To illustrate this point consider the case of an adjacent channel signal

$$f_m^{(n)}(t) \cos (\omega_o + \Delta)t$$

which is interfering with the reception of the desired signal

$$f_m(t) \cos \omega_o t.$$

In such a case the receiver input, $f_i(t)$, would be given by

$$f_i(t) = f_m(t) \cos \omega_o t + f_m^{(n)}(t) \cos (\omega_o + \Delta)t. \tag{102}$$

First using synchronous detection in the ordinary way we get

$$f_i(t) \cos \omega_o t \Big]_{L.P.} = \frac{f_m(t)}{2} + \frac{f_m^{(n)}(t)}{2} \cos \Delta t \tag{103}$$

which is the desired message plus a noise term due to the adjacent channel signal. This message, plus noise output, could be filtered for best message recovery by the single time series methods of Secs. II and III. However, if a sine detection is also made one obtains

$$f_i(t) \sin \omega_o t \Big]_{L.P.} = -\frac{f_m^{(n)}(t)}{2} \sin \Delta t. \tag{104}$$

This sine detection process yields no message voltage, but it does give a noise voltage which is correlated to the noise component of the cosine detector output (103). We may take advantage of the crosscorrelation between the voltage (104) and the noise component of (103) for best message recovery by the methods of Secs. II and III using the double time series results. A more general treatment of noise correlation in two-phase detection is given in the following section.

B. Two-Channel Analogy of a Radio Transmission Circuit

One possible method of transmitting a single message in a radio-frequency channel is illustrated by Fig. 6. The message, $f_m(t)$, amplitude modulates a cosine carrier directly while a sine carrier is modulated by $f_c(t)$, the output of a linear system $H(\omega)$ whose input is $f_m(t)$. To the transmitted signal $f_s(t)$, a noise voltage $f_n(t)$ is introduced additively in the transmission path so that the receiver input, $f_i(t)$, is equal to the sum of $f_s(t)$ and $f_n(t)$. Cosine and sine synchronous detection is then performed at the receiver, the $2\omega_o$ terms being removed by the low-pass filters $Q(\omega)$. Except for the removal of these high radio-frequency terms, the networks $Q(\omega)$ serve no other purpose. The actual filtering of the message from noise is performed by networks $H_{11}(\omega)$ and $H_{12}(\omega)$.

Since the input to $H_{11}(\omega)$ is $f_m(t) + g_1(t)$ and the input to $H_{12}(\omega)$ is $f_o(t) + g_2(t)$ the equivalent two-channel representation of Fig. 7 may be used rather than Fig. 6. The disturbance voltages $g_1(t)$ and $g_2(t)$ must now be determined from the actual representation of Fig. 6, for use in the equivalent representation of Fig. 7.

From Fig. 6 we have

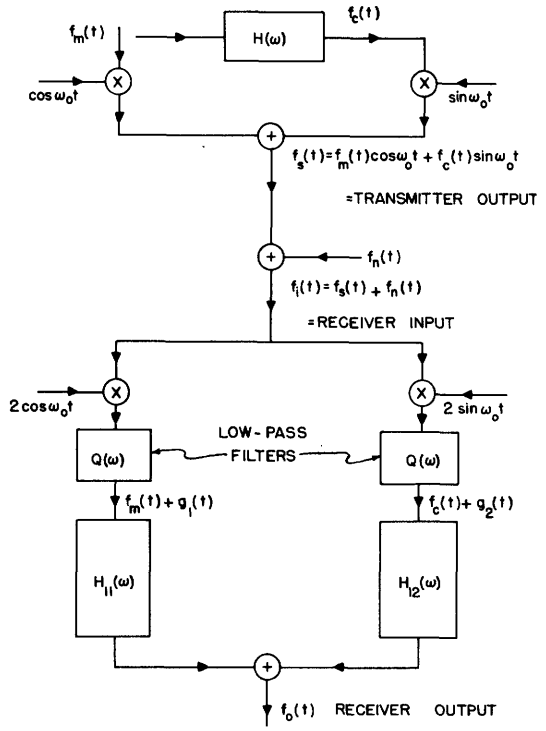

Fig. 6
A-m radio transmission circuit.

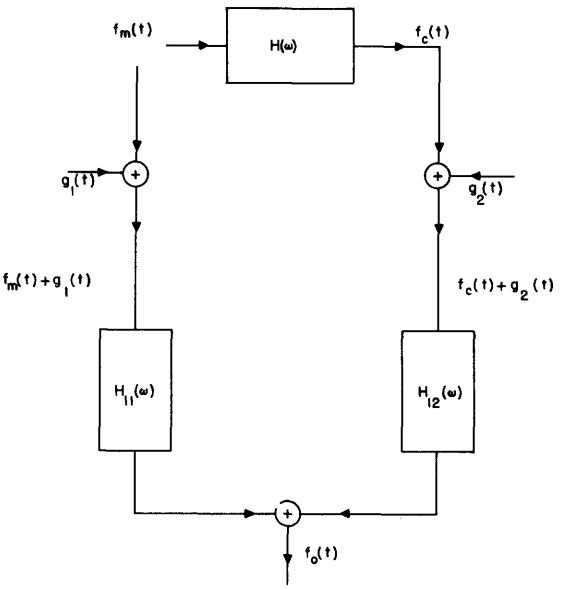

Fig. 7
Simplified equivalent transmission circuit.

$$g_1(t) = \int_{-\infty}^{\infty} d\sigma\, q(\sigma) 2 \cos\omega_o(t-\sigma) f_n(t-\sigma) \tag{105}$$

and

$$g_2(t) = \int_{-\infty}^{\infty} d\nu\, q(\nu) 2 \sin\omega_o(t-\nu) f_n(t-\nu). \tag{106}$$

These two voltages have the same autocorrelation functions, that is

$$\phi_{11}^{dd}(\tau) = \phi_{22}^{dd}(\tau) = \phi_{dd}(\tau) \tag{107}$$

where

$$\phi_{dd}(\tau) = \int_{-\infty}^{\infty}\int_{-\infty}^{\infty} d\sigma\, d\nu\, q(\sigma) q(\nu) 2\phi_{nn}(\tau+\sigma-\nu) \cos\omega_o(\tau+\sigma-\nu). \tag{108}$$

The disturbance power spectrum is then given by

$$\Phi_{dd}(\omega) = |Q(\omega)|^2 \left[\Phi_{nn}(\omega - \omega_o) + \Phi_{nn}(\omega + \omega_o)\right]. \tag{109}$$

The crosscorrelation between $g_1(t)$ and $g_2(t)$, $\phi_{12}^{dd}(\tau)$, is given by

$$\phi_{12}^{dd}(\tau) = \int_{-\infty}^{\infty}\int_{-\infty}^{\infty} d\sigma\, d\nu\, q(\sigma)q(\nu) 2\phi_{nn}(\tau+\sigma-\nu)\, \sin \omega_o(\tau+\sigma-\nu) \tag{110}$$

from which the cross-power spectrum

$$\Phi_{12}^{dd}(\omega) = \frac{|Q(\omega)|^2}{j}\left[\Phi_{nn}(\omega - \omega_o) - \Phi_{nn}(\omega + \omega_o)\right] \tag{111}$$

may be obtained. Thus, unless the noise in the radio channel, $f_n(t)$, has a spectrum $\Phi_{nn}(\omega)$ which is symmetric about ω_o there will always exist some correlation between $g_1(t)$ and $g_2(t)$.

In order to design the receiver filter networks $H_{11}(\omega)$ and $H_{12}(\omega)$ we have need for the following quantities as defined in Sec. II.

$$\Phi_{11}(\omega) = \Phi_{mm}(\omega) + \Phi_{dd}(\omega) \tag{112}$$

$$\Phi_{12}(\omega) = H(\omega)\Phi_{mm}(\omega) + \Phi_{12}^{dd}(\omega) \tag{113}$$

$$\Phi_{22}(\omega) = |H(\omega)|^2\Phi_{mm}(\omega) + \Phi_{dd}(\omega) \tag{114}$$

$$\Psi_{11}(\omega) = \Phi_{mm}(\omega) \tag{115}$$

$$\Psi_{21}(\omega) = H(-\omega)\Phi_{mm}(\omega). \tag{116}$$

For long-delay filtering (62) results in

$$H'_{11}(\omega) = \frac{\Phi_{mm}(\omega)\left[\Phi_{dd}(\omega) - H(-\omega)\Phi_{12}^{dd}(\omega)\right]}{D(\omega)} \tag{117}$$

while (63) gives

$$H'_{12}(\omega) = \frac{\Phi_{mm}(\omega)\left[H(-\omega)\Phi_{dd}(\omega) - \Phi_{12}^{dd}(-\omega)\right]}{D(\omega)} \tag{118}$$

where

$$\begin{aligned} D(\omega) = {} & \Phi_{mm}(\omega)\left\{\Phi_{dd}(\omega)\left[1 + |H(\omega)|^2\right] - H(\omega)\Phi_{12}^{dd}(-\omega) - H(-\omega)\Phi_{12}^{dd}(\omega)\right\} \\ & + \left\{\Phi_{dd}^2(\omega) - \left|\Phi_{12}^{dd}(\omega)\right|^2\right\}. \end{aligned} \tag{119}$$

The irremovable error of the transmission circuit may be obtained by substituting (118) and (119) into (67) which results in

$$\mathcal{E}_{irr} = \int_{-\infty}^{\infty} \frac{\Phi_{mm}(\omega)\left\{\Phi_{dd}^2(\omega) - \left|\Phi_{12}^{dd}(\omega)\right|^2\right\}}{D(\omega)}\, d\omega. \tag{120}$$

C. Double-Sideband Transmission and Reception

If $H(\omega)$ in Fig. 6 is chosen equal to zero, the transmitted signal, $f_s(t)$, will be simply

$$f_s(t) = f_m(t) \cos \omega_o t \tag{121}$$

which is an ordinary double-sideband a-m signal. This corresponds to putting all the signal power into channel one of Fig. 7 and using channel two for noise pickup only. For double-sideband (117) and (118) give

$$H'_{11}(\omega) = \frac{\Phi_{mm}(\omega)\Phi_{dd}(\omega)}{\Phi_{mm}(\omega)\Phi_{dd}(\omega) + \Phi^2_{dd}(\omega) - |\Phi^{dd}_{12}(\omega)|^2} \tag{122}$$

and

$$H'_{12}(\omega) = \frac{\Phi_{mm}(\omega)\Phi^{dd}_{12}(\omega)}{\Phi_{mm}(\omega)\Phi_{dd}(\omega) + \Phi^2_{dd}(\omega) - |\Phi^{dd}_{12}(\omega)|^2}. \tag{123}$$

The irremovable error as given by (120) becomes

$$\mathcal{E}_{\substack{irr \\ DSB}} = \int_{-\infty}^{\infty} \frac{\Phi_{mm}(\omega)\left\{\Phi^2_{dd}(\omega) - |\Phi^{dd}_{12}(\omega)|^2\right\}}{\Phi_{mm}(\omega)\Phi_{dd}(\omega) + \Phi^2_{dd}(\omega) - |\Phi^{dd}_{12}(\omega)|^2}\, d\omega. \tag{124}$$

D. Single-Sideband Transmission and Reception

Let $H(\omega)$ in Fig. 6 be defined by

$$\left.\begin{aligned} H(\omega) &= +j \quad \text{for } \omega > 0 \\ H(\omega) &= -j \quad \text{for } \omega < 0. \end{aligned}\right\} \tag{125}$$

In this discussion we shall ignore the infinite delay associated with the response of (125). The transmitted signal will then be

$$f_s(t) = f_m(t) \cos \omega_o t + f_c(t) \sin \omega_o t \tag{126}$$

where

$$f_c(t) = \int_{-\infty}^{\infty} d\sigma\, h(\sigma) f_m(t-\sigma). \tag{127}$$

The signal autocorrelation function will be given by

$$\phi_{ss}(\tau) = \frac{\cos \omega_o \tau}{2}\left[\phi_{mm}(\tau) + \phi_{cc}(\tau)\right] + \frac{\sin \omega_o \tau}{2}\left[\phi_{mc}(\tau) - \phi_{cm}(\tau)\right]. \tag{128}$$

Now since

$$\Phi_{cc}(\omega) = |H(\omega)|^2\, \Phi_{mm}(\omega) = \Phi_{mm}(\omega) \tag{129}$$

and

$$\Phi_{mc}(\omega) = H(\omega)\Phi_{mm}(\omega) = \Phi_{cm}(-\omega) \tag{130}$$

the power spectrum of the transmitted signal becomes

$$\Phi_{ss}(\omega) = \frac{1}{2}\left[\Phi_{mm}(\omega - \omega_o) + \Phi_{mm}(\omega + \omega_o)\right] + \frac{1}{4j}\left\{\left[H(\omega - \omega_o) - H(-\omega + \omega_o)\right]\Phi_{mm}(\omega - \omega_o)\right.$$

$$\left. + \left[H(-\omega - \omega_o) - H(\omega + \omega_o)\right]\Phi_{mm}(\omega + \omega_o)\right\}. \tag{131}$$

Therefore

$$\left.\begin{aligned} \Phi_{ss}(\omega) &= \Phi_{mm}(\omega - \omega_o) && \text{for } \omega > \omega_o \\ \Phi_{ss}(\omega) &= 0 && \text{for } -\omega_o < \omega < \omega_o \\ \Phi_{ss}(\omega) &= \Phi_{mm}(\omega + \omega_o) && \text{for } \omega < -\omega_o. \end{aligned}\right\} \tag{132}$$

From Fig. 8 it can be seen that a single-sideband transmitted signal results if $H(\omega)$ is chosen as in (125). If the +j and -j terms of (125) are interchanged, the signal will again be single-sideband, but with the lower sideband being transmitted.

Using the results of Sec. IV-B, it may be shown that

$$H'_{11}(\omega)_{\omega>0} = \frac{\Phi_{mm}(\omega)}{2\Phi_{mm}(\omega) + \Phi_{dd}(\omega) + j\Phi_{12}^{dd}(-\omega)} \tag{133}$$

$$H'_{12}(\omega)_{\omega>0} = \frac{-j\Phi_{mm}(\omega)}{2\Phi_{mm}(\omega) + \Phi_{dd}(\omega) + j\Phi_{12}^{dd}(-\omega)} = -jH'_{11}(\omega)_{\omega>0} \tag{134}$$

and that

$$\mathcal{E}_{\substack{irr \\ SSB+}} = 2\int_0^\infty \frac{\Phi_{mm}(\omega)\left[\Phi_{dd}(\omega) - j\Phi_{12}^{dd}(\omega)\right]}{2\Phi_{mm}(\omega) + \Phi_{dd}(\omega) - j\Phi_{12}^{dd}(\omega)}\, d\omega. \tag{135}$$

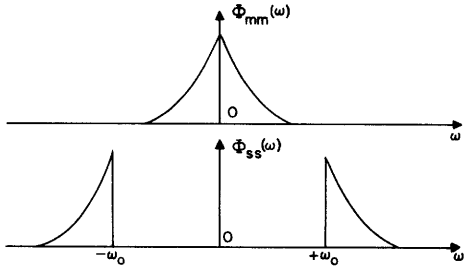

Fig. 8
(top) Original message spectrum.
(bottom) Resultant single-sideband signal spectrum.

Since single-sideband and double-sideband systems are to be compared in the next section a few changes must be made in the error expressions to insure a fair comparison. From (128) it can be seen that the transmitted average power is $2\phi_{mm}(0)$ while for the double-sideband case (121) shows an average power of $\phi_{mm}(0)$. Thus, in order to have the same power in both cases we must replace $\Phi_{mm}(\omega)$ in (135) by $\Phi_{mm}(\omega)/2$. This corresponds to dividing $f_m(t)$ by $\sqrt{2}$ and since the system is now minimizing the mean-square error

between $f_o(t)$ and $f_m(t)/\sqrt{2}$ we must multiply the resulting $\mathcal{E}_{irr}$ expression by two to regain the voltage level assumed by (124). When these changes are made we have for upper-sideband transmission

$$\mathcal{E}_{\substack{irr \\ SSB+}} = 2 \int_0^\infty \frac{\Phi_{mm}(\omega) \left[\Phi_{dd}(\omega) - j\Phi_{12}^{dd}(\omega)\right]}{\Phi_{mm}(\omega) + \Phi_{dd}(\omega) - j\Phi_{12}^{dd}(\omega)} d\omega \tag{136}$$

and for lower-sideband transmission

$$\mathcal{E}_{\substack{irr \\ SSB-}} = 2 \int_0^\infty \frac{\Phi_{mm}(\omega) \left[\Phi_{dd}(\omega) + j\Phi_{12}^{dd}(\omega)\right] d\omega}{\Phi_{mm}(\omega) + \Phi_{dd}(\omega) + j\Phi_{12}^{dd}(\omega)}. \tag{137}$$

The double-sideband error equation (124) may be written as

$$\mathcal{E}_{\substack{irr \\ DSB}} = 2 \int_0^\infty \frac{\Phi_{mm}(\omega) \left\{\Phi_{dd}^2(\omega) - |\Phi_{12}^{dd}(\omega)|^2\right\} d\omega}{\Phi_{mm}(\omega)\Phi_{dd}(\omega) + \Phi_{dd}^2(\omega) - |\Phi_{12}^{dd}(\omega)|^2}. \tag{138}$$

E. Adjacent Channel Interference Studies

If the radio-frequency channel noise, $f_n(t)$, is "white" then

$$\Phi_{nn}(\omega) = a^2 \tag{139}$$

and from (109) and (111) we have

$$\Phi_{dd}(\omega) = 2a^2 \tag{140}$$

and

$$\Phi_{12}^{dd}(\omega) = 0. \tag{141}$$

Under these conditions (136), (137), and (138) become identical. Thus, for white noise in the radio channel single-sideband and double-sideband systems will give identical performance. In many practical situations the main cause of trouble is not white noise but rather adjacent channel interference. For example, if the interfering signal is a nearby a-m signal $f_n(t)$ will be given by

$$f_n(t) = f_m^{(n)}(t) \cos(\omega_o + \Delta)t \tag{142}$$

which will result in

$$\Phi_{dd}(\omega) = \frac{1}{4}\left[\Phi_{mm}^{nn}(\omega-\Delta) + \Phi_{mm}^{nn}(\omega+\Delta)\right] \tag{143}$$

and

$$\Phi_{12}^{dd}(\omega) = \frac{1}{4j}\left[\Phi_{mm}^{nn}(\omega+\Delta) - \Phi_{mm}^{nn}(\omega-\Delta)\right]. \tag{144}$$

Equations (143) and (144) are valid for both $\Delta > 0$ and $\Delta < 0$.

If the interference is caused by a single-sideband signal transmitting the upper sideband, we shall have

$$f_n(t) = f_m^{(n)}(t) \cos(\omega_o + \Delta)t + f_c^{(n)}(t) \sin(\omega_o + \Delta)t \tag{145}$$

where $f_m^{(n)}(t)$ and $f_c^{(n)}(t)$ are related by $H(\omega)$ of (125) and Fig. 6. Using now (131), (109), and (111) we obtain for $\Delta > 0$

$$\left.\begin{aligned} \Phi_{dd}(\omega) &= \Phi_{mm}^{nn}(\omega-\Delta) && \text{for } \omega > \Delta \\ \Phi_{dd}(\omega) &= 0 && \text{for } -\Delta < \omega < \Delta \\ \Phi_{dd}(\omega) &= \Phi_{mm}^{nn}(\omega+\Delta) && \text{for } \omega < -\Delta \end{aligned}\right\} \tag{146}$$

and

$$\left.\begin{aligned} \Phi_{12}^{dd}(\omega) &= -\frac{1}{j}\Phi_{mm}^{nn}(\omega-\Delta) && \text{for } \omega > \Delta \\ \Phi_{12}^{dd}(\omega) &= 0 && \text{for } -\Delta < \omega < \Delta \\ \Phi_{12}^{dd}(\omega) &= \frac{1}{j}\Phi_{mm}^{nn}(\omega+\Delta) && \text{for } \omega < -\Delta . \end{aligned}\right\} \tag{147}$$

If $\Delta < 0$ we let $\delta = -\Delta$ and obtain in the same manner

$$\left.\begin{aligned} \Phi_{dd}(\omega) &= \Phi_{mm}^{nn}(\omega+\delta) && \text{for } \omega > \delta \\ \Phi_{dd}(\omega) &= \Phi_{mm}^{nn}(\omega-\delta) + \Phi_{mm}^{nn}(\omega+\delta) && \text{for } -\delta < \omega < \delta \\ \Phi_{dd}(\omega) &= \Phi_{mm}^{nn}(\omega-\delta) && \text{for } \omega < -\delta \end{aligned}\right\} \tag{148}$$

and

$$\left.\begin{aligned} \Phi_{12}^{dd}(\omega) &= \frac{-1}{j}\Phi_{mm}^{nn}(\omega+\delta) && \text{for } \omega > \delta \\ \Phi_{12}^{dd}(\omega) &= \frac{1}{j}\left[\Phi_{mm}^{nn}(\omega-\delta) - \Phi_{mm}^{nn}(\omega+\delta)\right] && \text{for } -\delta < \omega < \delta \\ \Phi_{12}^{dd}(\omega) &= \frac{1}{j}\Phi_{mm}^{nn}(\omega-\delta) && \text{for } \omega < -\delta . \end{aligned}\right\} \tag{149}$$

Using the results of this section we may now consider certain special interference situations.

(1) Desired signal DSB, undesired signal DSB.

In this case (138), (129), and (146) must be used yielding

$$\mathcal{E}_{\substack{\text{irr}\\\text{DSB}}} = 2\int_0^\infty \frac{d\omega}{\frac{1}{\Phi^{nn}_{mm}(\omega+\Delta)} + \frac{1}{\Phi^{nn}_{mm}(\omega-\Delta)} + \frac{1}{\Phi_{mm}(\omega)}}. \tag{150}$$

Let us assume that $f_m(t)$ and $f_m^{(n)}(t)$ have spectra which are related by

$$\Phi^{nn}_{mm}(\omega) = K\Phi_{mm}(\omega). \tag{151}$$

Thus

$$K = \frac{\text{Average Power of Undesired Signal}}{\text{Average Power of Desired Signal}}. \tag{152}$$

Let us further assume that

$$\Phi_{mm}(\omega) = \frac{\beta}{\pi} \times \frac{1}{\omega^2 + \beta^2}. \tag{153}$$

When (153) and (151) are substituted into (150) one obtains

$$\mathcal{E}_{\text{irr}} = \frac{K}{\sqrt{2+K}} \times \frac{1}{\sqrt{(2+K) + 2\left(\frac{\Delta}{\beta}\right)^2}}. \tag{154}$$

It is interesting to compare (154) with the error expression obtained if the sine detection as shown in Fig. 6 had not been performed. The expression for single-phase detection may be shown to be

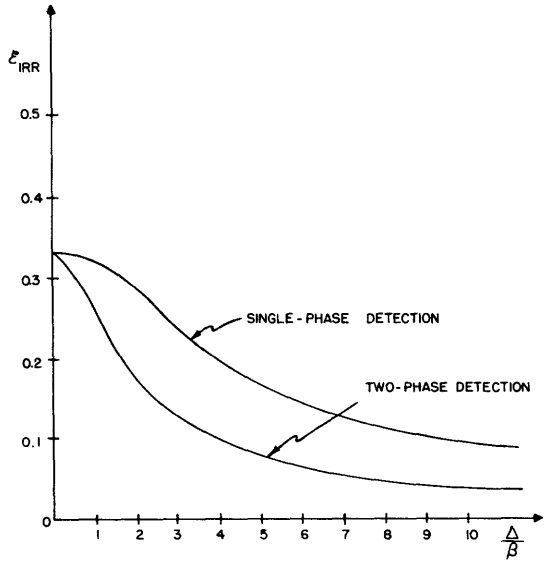

Fig. 9

Adjacent channel interference: desired and undesired signals DSB.

$$\mathcal{E}_{\text{irr}} = \frac{K\left[\left(1 + \frac{\Delta^2}{\beta^2}\right)\sqrt{r} + \frac{\sqrt{p}}{\beta^2}\right]}{\left(\frac{q}{\beta^2} + 2\frac{\sqrt{pr}}{\beta^2}\right)^{1/2}\frac{\sqrt{pr}}{\beta^2}} \tag{155}$$

where

$$\left.\begin{aligned} \frac{p}{\beta^4} &= \left(1 + \frac{\Delta^2}{\beta^2}\right)\left[(K+2) + 2\frac{\Delta^2}{\beta^2}\right] \\ \frac{q}{\beta^2} &= \left[2(K+2) + (K-4)\frac{\Delta^2}{\beta^2}\right] \\ r &= (K+2). \end{aligned}\right\} \tag{156}$$

Equations (154) and (155) are plotted for comparison in Fig. 9 for K = 1. Note that for a given mean-square error single-phase detection requires about twice the center

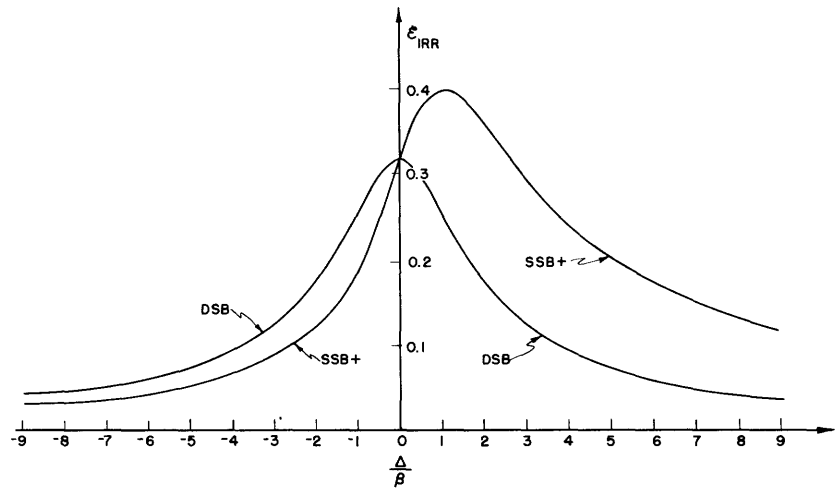

Fig. 10

Adjacent channel interference:
undesired signal DSB; desired signal as indicated.

frequency separation of two-phase detection. For example, if $\mathcal{E}_{irr} = 0.2$, $\Delta \cong 1.6\beta$ for two-phase detection while a separation of $\Delta \cong 4\beta$ is required if cosine detection only is used.

(2) Desired signal SSB+, undesired signal DSB.

Substituting (143) and (144) into (136) while using (151) and (153) will yield

$$\mathcal{E}_{\substack{irr \\ SSB+}} = \frac{\frac{2K}{\pi}}{\sqrt{(K+2)^2 + 2a^2K}} \left[\frac{\pi}{2} + \tan^{-1} \frac{2a}{\sqrt{(K+2)^2 + 2a^2K}}\right] \tag{157}$$

where $a = \Delta/\beta$. In Fig. 10 (157) and (154) are plotted for comparison for $K = 1$.

(3) Desired signal SSB+, undesired signal SSB+.

In keeping with the conditions which led from (135) to (136) we must divide (146) and (147) by two before substituting into (136). This gives for $\Delta > 0$

$$\mathcal{E}_{\substack{irr \\ SSB+}} = 2 \int_{\Delta}^{\infty} \frac{\Phi_{mm}(\omega)\Phi^{nn}_{mm}(\omega-\Delta)d\omega}{\Phi_{mm}(\omega) + \Phi^{nn}_{mm}(\omega-\Delta)}. \tag{158}$$

After applying (151) and (153) we get

$$\mathcal{E}_{\substack{irr \\ SSB+}} = \frac{\frac{2K}{\pi}}{\sqrt{K(a^2+2) + K^2 + 1}} \left[\frac{\pi}{2} - \tan^{-1} \frac{Ka}{\sqrt{K(a^2+2) + K^2 + 1}}\right] \tag{159}$$

where $a = \Delta/\beta$ and $\Delta > 0$.

For $\Delta < 0$ use (148) and (149) obtaining

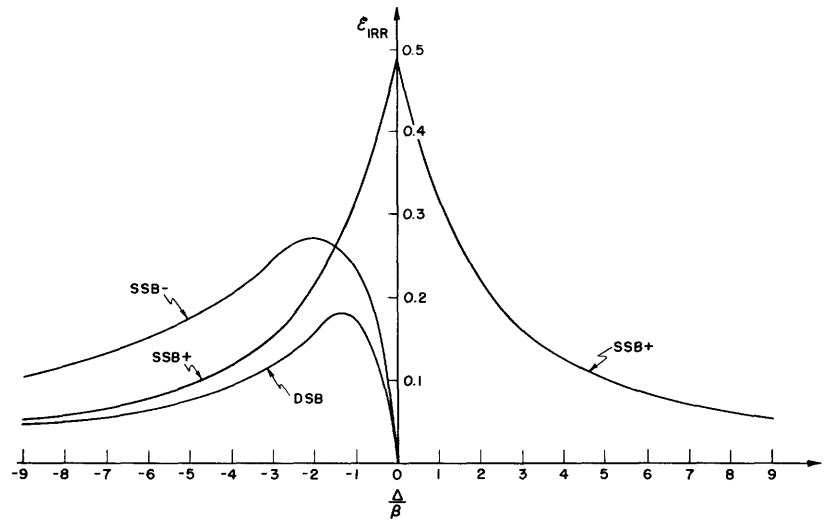

Fig. 11

Adjacent channel interference:
undesired signal SSB+; desired signal as indicated.

$$\mathcal{E}_{\substack{irr \\ SSB+}} = \frac{\frac{2K}{\pi}}{\sqrt{K(a^2+2)+K^2+1}}\left[\frac{\pi}{2} - \tan^{-1}\frac{a}{\sqrt{K(a^2+2)+K^2+1}}\right] \tag{160}$$

where $a = -\Delta/\beta$ and $\Delta < 0$. Equations (159) and (160) are plotted in Fig. 11 for K = 1.

(4) Desired signal SSB-, undesired signal SSB+.

When (146) and (147) are substituted into (137) one gets

$$\mathcal{E}_{\substack{irr \\ SSB-}} = 0 \text{ for } \Delta > 0 \tag{161}$$

as expected. For $\Delta < 0$ dividing (148) and (149) by two and using (137) one obtains

$$\mathcal{E}_{\substack{irr \\ SSB-}} = \frac{\frac{2K}{\pi}}{\sqrt{K(a^2+2)+K^2+1}}\left[\tan^{-1}\frac{Ka}{\sqrt{K(a^2+2)+K^2+1}} + \tan^{-1}\frac{a}{\sqrt{K(a^2+2)+K^2+1}}\right] \tag{162}$$

where $a = -\Delta/\beta$ and $\Delta < 0$. Equation (162) is plotted in Fig. 11 for K = 1.

(5) Desired signal DSB, undesired signal SSB+.

For $\Delta > 0$ substitution of (146) and (147) into (138) yields

$$\mathcal{E}_{\substack{irr \\ DSB}} = 0 \text{ for } \Delta > 0. \tag{163}$$

For $\Delta < 0$ dividing (148) and (149) by two and substituting into (138) yields

$$\mathcal{E}_{\substack{irr \\ DSB}} = \frac{2K}{\pi}\frac{1}{\sqrt{(K+1)\left[(K+1)+a^2\right]}}\tan^{-1} a\sqrt{\frac{K+1}{K+1+a^2}} \tag{164}$$

where $\alpha = -\Delta/\beta$ and $\Delta < 0$. Equations (163) and (164) are plotted for $K = 1$ in Fig. 11. Note that (163) holds even though the upper sideband power is being used by the receiver.

F. Summary of Results

One difficulty with synchronous detection is the need for phase synchronization in the receiver. That is, we must generate a pair of local signals which not only must be of the correct frequency, but must also be of the correct phase with respect to the desired signal. On the other hand the envelope type of detectors now in general use are not phase or even frequency sensitive. However, these properties which make the envelope detector easy to use are the same properties which make it an inferior performer. The following list of advantages of synchronous over envelope detection serves to clarify this last statement.

(1) Use of synchronous detection allows filtering to be performed after detection. This makes possible use of broad banded inputs with subsequent elimination of tracking problems. Also since the filtering may be done at audio frequencies more flexibility in filter design is available to meet various different interference situations.

(2) In the case of adjacent channel interference the S/N power ratio after detection is exactly twice the S/N ratio before detection as may be observed from (102) and (103). This is a result of the frequency discrimination characteristic which is totally lacking when envelope detection is used.

(3) The phase-sensitive property of synchronous detectors makes possible the "phase-duplexing" of two messages in a given channel as discussed in Sec. IV-A. This is clearly impossible when using envelope detection.

(4) Synchronous detection makes possible the use of two-channel interference filtering techniques for improved message recovery as demonstrated by Fig. 9. Even in the case of white noise disturbance where noise crosscorrelation vanishes, it can be shown that synchronous detection is superior to envelope detection for low S/N ratios. For high S/N ratios the two detectors will give about the same results.

(5) The presence of a carrier wave is not needed when synchronous detection is used whereas a full carrier must be transmitted for envelope detection. As a practical matter a low level carrier might be transmitted for purposes of synchronization and for information concerning the transmission medium, but the greater part of the power of the full carrier could be used in the sidebands for more effective transmission.

With the above advantages in mind it is interesting to compare single-sideband and double-sideband systems when both are being properly received. From Figs. 10 and 11 it can be seen that in almost every case DSB operation is superior to SSB operation. This may seem strange since the DSB signal occupies twice the bandwidth of the SSB signal. However, consider the equivalent transmission circuit of Fig. 7. In Sec. IV-C it was shown that DSB transmission results in the sending of all the signal energy down channel one and using channel two only for noise pickup. Section IV-D shows that in the SSB case half the signal energy is sent down each line. Since networks $H_{11}(\omega)$ and $H_{12}(\omega)$ in the SSB case both receive signal power, a design compromise must be made

for best signal reinforcement consistent with best noise cancellation. In the DSB case only $H_{11}(\omega)$ receives signal power and in general a better job of filtering may be done.

Another point to consider here is the fact that when nonlinear operations are performed spectrum functions tell only part of the story. For example in the phase duplexing situation of Sec. IV-A we may have two signals with identical spectra and yet separate them perfectly by the two-phase detection method described previously.

V. Examples of the Use of the Approximation Method and Experimental Results

A. Synthesis of Transfer Functions

At the end of Sec. III the problem of designing networks having transfer functions of the form (90) was discussed. It was proposed that impedances Z_1 and Z_2 of (92) be built and used in the manner of Fig. 4 in order to obtain the desired transfer function. The circuit diagram of an electronic filter based on Fig. 4 is shown in Fig. 12 and described below.

The filter input voltage is phase inverted by V-1, the outputs of which drive pentodes V-2 and V-3 in push-pull. Thus the plate currents of V-2 and V-3 are equal and proportional to the filter input voltage but opposite in sign. The networks Z_1 and Z_2 are plugged into the octal sockets directly above V-2 and V-3. Thus if the plate voltages of V-2 and V-3 are added, the desired transfer function will clearly result. The pentode V-4 acts as a constant current source and compensates for unequal tube drives and transconductances. This eliminates the need for any phase inverter adjustments or tube selection of V-2 and V-3.

The adder circuit cathode followers V-5 and V-6 have large cathode loads, thus making the gain very nearly unity and essentially independent of tube parameters. The two 100K resistors in the output circuit were matched to within one percent. Thus, the sum of plate voltages V-2 and V-3 appears across the grid resistor of the cathode follower output tube V-7.

B. Single Time Series

In order to demonstrate the approximation method for the single time series case we choose a message correlation function $\phi_{mm}(\tau)$ where

$$\phi_{mm}(\tau) = \pi\epsilon^{-\beta|\tau|} \tag{165}$$

and a noise correlation function $\phi_{nn}(\tau)$ where

$$\phi_{nn}(\tau) = 2\pi a^2 u_o(\tau). \tag{166}$$

Zero crosscorrelation is assumed between the message and noise. The resulting power density spectra are

$$\Phi_{mm}(\omega) = \frac{\beta}{\omega^2 + \beta^2} \tag{167}$$

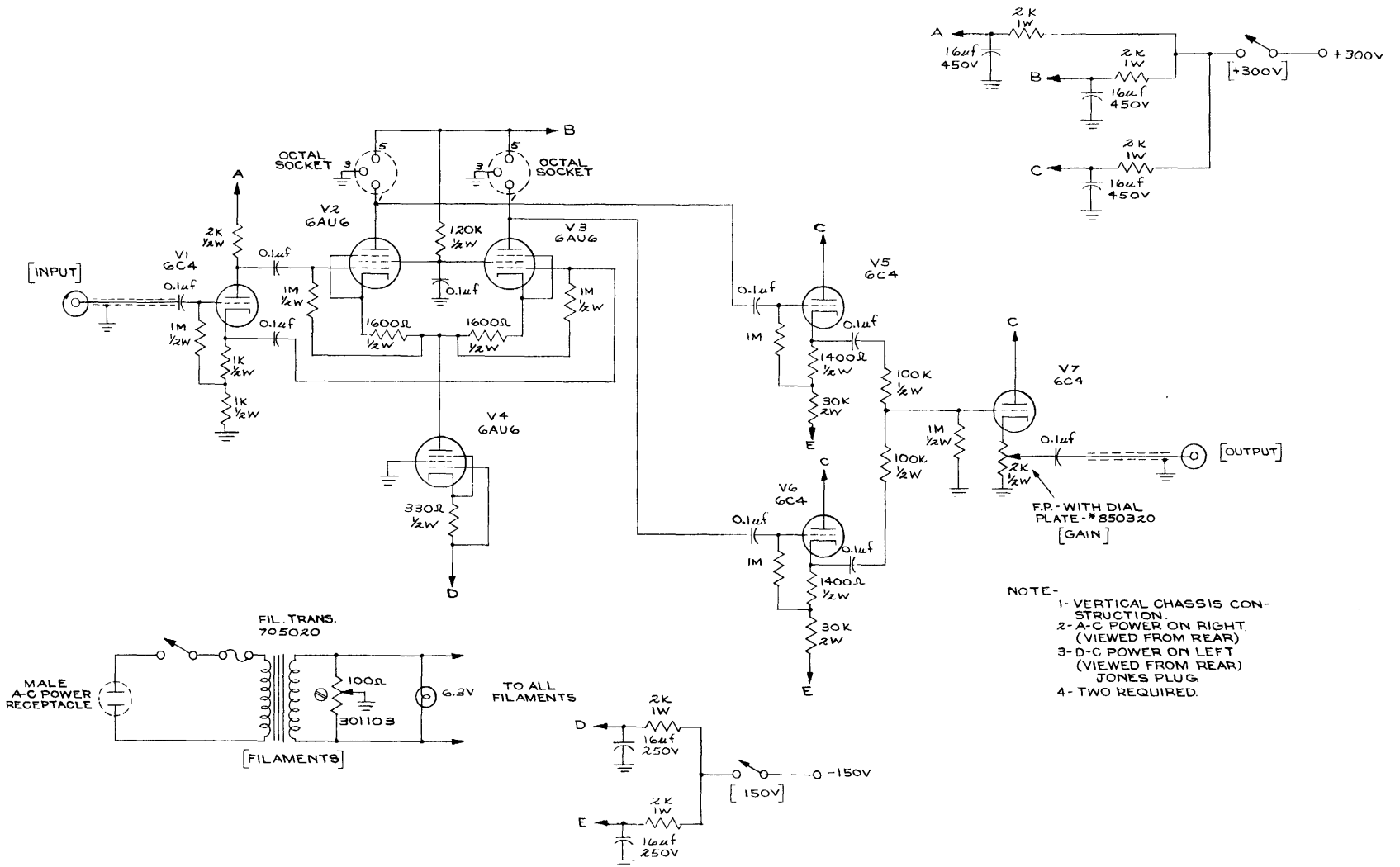

Fig. 12

Electronic filter circuit diagram.

and

$$\Phi_{nn}(\omega) = a^2. \tag{168}$$

From Sec. III using (86) for the case n=1 we have

$$\sum_{u=1}^{N} c_u^{11} B_{su} = A_s, \qquad (1 \leqslant s \leqslant N) \tag{169}$$

and from (87)

$$\mathcal{E}_{min} = \phi_{11}^{mm}(0) - \sum_{s=1}^{N} c_s^{11} A_s \tag{170}$$

where

$$B_{su} = \int_0^\infty \int_0^\infty d\sigma d\nu \phi_{11}(\sigma - \nu) \epsilon^{-sp\sigma} \epsilon^{-up\nu} \tag{171}$$

and

$$A_s = \int_0^\infty d\sigma \psi_{11}(\sigma \pm a) \epsilon^{-sp\sigma}. \tag{172}$$

When (165) and (166) are substituted into (171) and (172) there results for the lagging filter case

$$B_{su} = \frac{2\pi a^2}{p(u+s)} + \frac{\pi}{(\beta - pu)} \left[\frac{1}{p(s+u)} - \frac{1}{(ps + \beta)} \right] + \frac{\pi}{(\beta + pu)p(s+u)} \tag{173}$$

and

$$A_s = \pi \left\{ \frac{\epsilon^{-a\beta}}{(sp - \beta)} - \frac{2\beta \epsilon^{-asp}}{(sp + \beta)(sp - \beta)} \right\}. \tag{174}$$

Now if we let

$$\left.\begin{array}{ll} a^2 = 0.25 & \beta = 1 \\ p = 1 & a = 0.5 \end{array}\right\} \tag{175}$$

and solve (169) the results obtained will be as shown in Table I. When the coefficients from this table are used in (76) the resulting network impulse responses are obtained. Plots of these responses for the different N are shown in Fig. 13 along with the ideal response (ref. 6).

Note from Table I that for N=3 the mean-square error of filtering is very nearly equal to $\mathcal{E}_{min}$ for the ideal response. The response curves for N=3, 4, 5 are very nearly the same as are the $\mathcal{E}_{min's}$ for these values of N. For N=6 some difference may be noted in the response curve but very little improvement results in the value of $\mathcal{E}_{min}$ over that for N=3.

Table I

N	1	2	3	4	5	6
c_1^{11}	0.80871	0.76982	-0.47011	-0.45640	-0.45787	-0.3941
c_2^{11}		0.06562	5.7515	5.63304	5.66315	4.014
c_3^{11}			-5.11066	-4.85417	-4.9950	1.643
c_4^{11}				-0.15746	0.06815	-5.2668
c_5^{11}					-0.11527	-6.0673
c_6^{11}						6.4192
$\mathcal{E}_{min}$	0.509π	0.509π	0.472π	0.472π	0.472π	0.470π
For ideal network, $\mathcal{E}_{min} = 0.465\pi$						

For an experimental check using the N=3 results we first change (175) to

$$\left.\begin{aligned} a^2 &= 0.25 \times 10^{-4} & \beta &= 10^4 \\ p &= 10^4 & \alpha &= 0.5 \times 10^{-4} \end{aligned}\right\} \qquad (176)$$

From (173) and (174) it can be seen that this change will result in an increase of the c_u^{11}

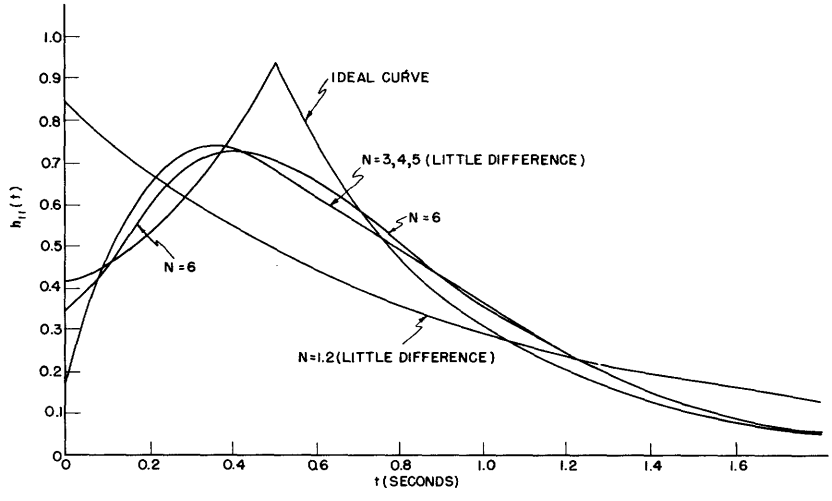

Fig. 13

Network impulse response: single time series.

of Table I by a factor of 10^4. Since a constant factor multiplication of this sort merely changes the impedance level of Z_1 and Z_2 it is of no consequence.

From Fig. 4 and (91) it can be seen that the R's and C's of z_1 and z_2 will be related to the c_u^{11} by

$$R_u = \frac{c_u^{11}}{pu} \tag{177}$$

and

$$C_u = \frac{1}{c_u^{11}}. \tag{178}$$

Of course the impedance level of the resulting networks may be changed so that practical R and C values will result.

Using the above results the following networks were obtained for N=3 of Table I using the values of (176).

The experimental test setup used is shown in Fig. 15 and photographs of the time functions involved are shown in Fig. 16. A random square wave having an average crossing rate of 5000 per second was used as the message (ref. 6) and a white noise generator produced the noise voltage. All the equipment of Fig. 15 except the electronic filter was designed and built by C. A. Stutt and a detailed description of these components may be found elsewhere (refs. 19, 20). The measured mean-square error was 0.51π and the calculated value from Table I is given as 0.472π. The difference between the calculated and measured $\mathcal{E}_{min}$ values is well within the range of experimental error.

C. Double Time Series

In this section we shall consider the design of networks $H_{11}(\omega)$ and $H_{12}(\omega)$ of Fig. 6 by the methods of Sec. III. In particular the case of adjacent channel interference between two double-sideband signals will be considered. The receiver input $f_i(t)$ will be given by

$$f_i(t) = f_m(t)\cos \omega_o t - f_m^{(n)}(t)\sin(\omega_o + \Delta)t. \tag{179}$$

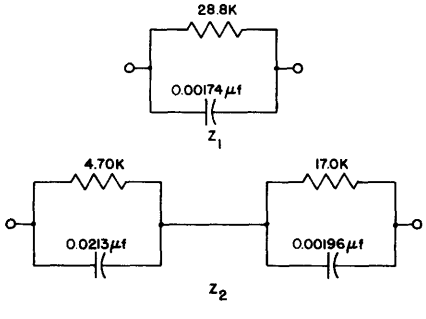

Fig. 14
Networks Z_1 and Z_2: single time series; N = 3.

After synchronous detection and low-pass filtering as shown in Fig. 6 we have for the input to $H_{11}(\omega)$

$$f_m(t) + f_m^{(n)}(t)\cos \Delta t$$

and for the input to $H_{12}(\omega)$ we have

$$f_m^{(n)}(t)\sin \Delta t.$$

Let $f_m(t)$ and $f_m^{(n)}(t)$ have the same autocorrelation function $\phi_{mm}(\tau)$ where

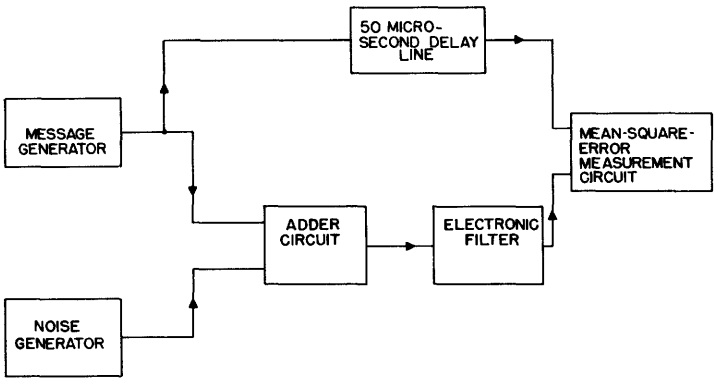

Fig. 15

Experimental test set-up: single time series.

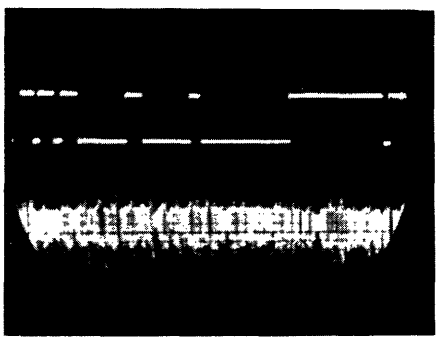

A- MESSAGE GENERATOR OUTPUT
B- NOISE GENERATOR OUTPUT

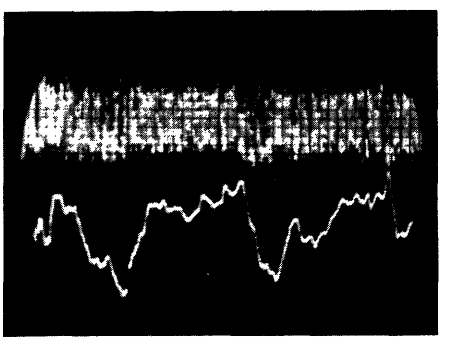

A- ELECTRONIC FILTER INPUT
B- ELECTRONIC FILTER OUTPUT

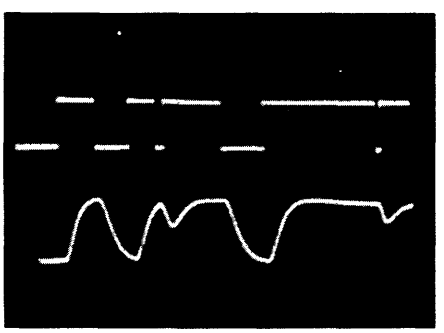

A- MESSAGE ONLY INTO ELECTRONIC FILTER
B- ELECTRONIC FILTER OUTPUT

A- UPPER TRACE
B- LOWER TRACE

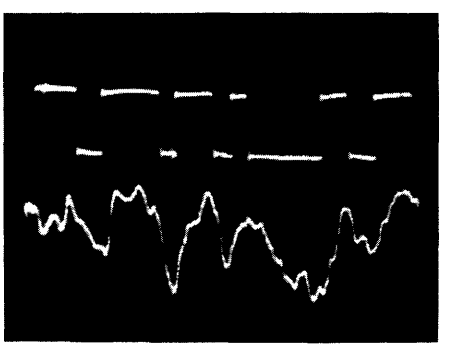

A- DELAY LINE OUTPUT
B- ELECTRONIC FILTER OUTPUT

TRACE DESCRIPTIONS REFER TO FIGURE 15

Fig. 16

Experimental test set-up oscillographs: single time series.

$$\phi_{mm}(\tau) = \epsilon^{-\beta|\tau|}. \tag{180}$$

Thus using the notation of Sec. II one obtains

$$\phi_{11}(\tau) = \epsilon^{-\beta|\tau|}\left(1 + \frac{\cos \Delta\tau}{2}\right) \tag{181}$$

$$\phi_{12}(\tau) = \epsilon^{-\beta|\tau|}\frac{\sin\Delta\tau}{2} \tag{182}$$

$$\phi_{22}(\tau) = \epsilon^{-\beta|\tau|}\frac{\cos\Delta\tau}{2} \tag{183}$$

$$\psi_{11}(\tau) = \epsilon^{-\beta|\tau|} \tag{184}$$

and

$$\psi_{21}(\tau) = 0. \tag{185}$$

For a delay filter solution we let

$$\left.\begin{aligned} a &= 10^{-4} \qquad p = 5 \times 10^{3} \\ \beta &= 10^{4} \qquad\quad = 2 \times 10^{4} \end{aligned}\right\} \tag{186}$$

and when (181) through (185) are substituted into (88) a set of 2N simultaneous equations result involving the c_u^{11} and c_u^{12} unknowns. Table II gives the coefficient solutions and $\mathcal{E}_{min}$ values for various N. A multiplier of 10^4 has been omitted in the table for reasons discussed in the previous section. The network impulse response functions $h_{11}(t)$ and $h_{12}(t)$ are plotted in Figs. 17 through 22 for different N values.

For experimental purposes an N value of 4 was chosen. Using the coefficient values from Table II, networks Z_1 and Z_2 were obtained for $H_{11}(\omega)$ and $H_{12}(\omega)$ as shown in Fig. 23. The message voltage $f_m(t)$ was produced by passing white noise through an RC filter having a half-power frequency of 1590 cps. For the noise voltage $f_m^{(n)}(t)$ a random square wave having an average of 5000 zero crossings per second was used. A block diagram of the experimental arrangement is shown in Fig. 24 with detailed circuit diagrams for the interference filtering test circuit and the amplifier-adder circuit being given by Figs. 25 and 26 respectively. The multiplier circuits V_4, V_5 and V_{13}, V_{14} are described in detail elsewhere (ref. 21). As in the single time series work the message and noise generators, delay line, and mean-square error measurement circuit were designed and built by C. A. Stutt and detailed descriptions of these units may be found in his writings (refs. 19, 20).

The measured value of $\mathcal{E}_{min}$ was found to be 0.39 while the calculated value from Table II is given as 0.32. Here again the discrepancy is well within experimental error. Photographs of some of the time functions involved are shown in Fig. 27.

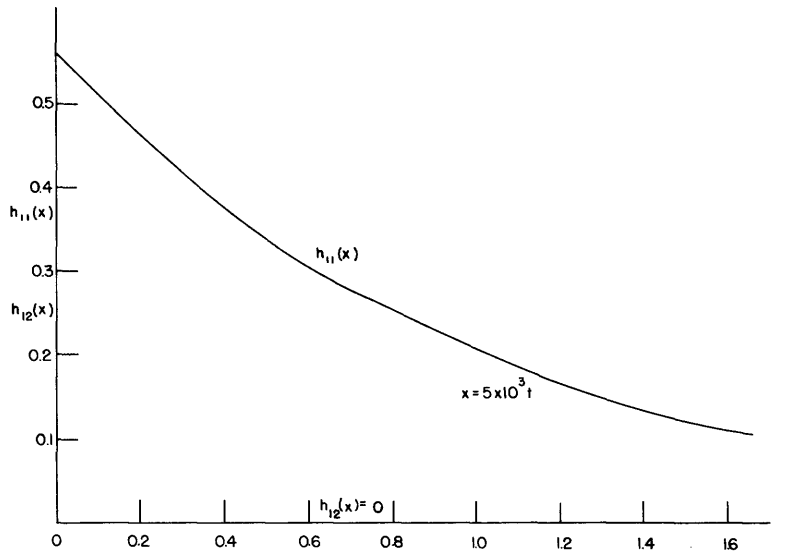

Fig. 17

Network impulse response:
double time series; N = 1.

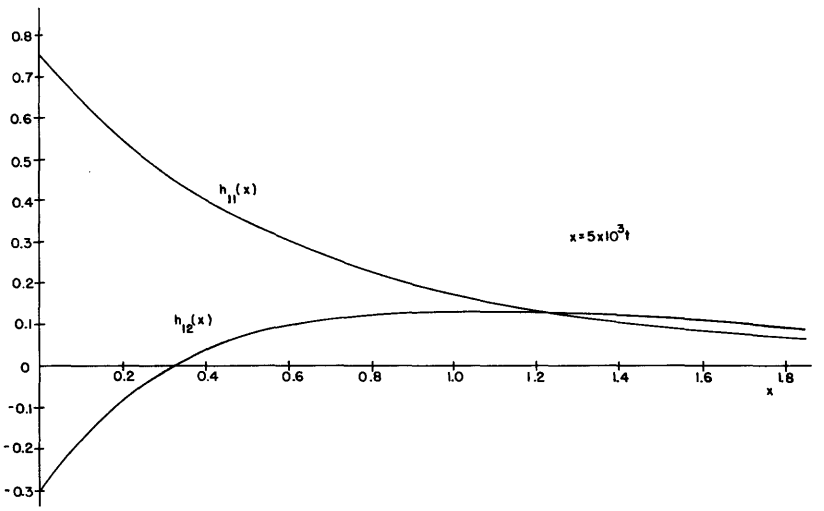

Fig. 18

Network impulse response:
double time series; N = 2.

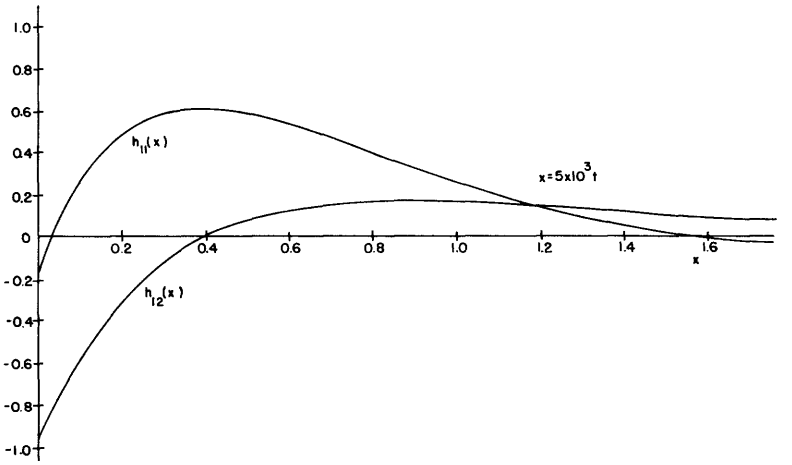

Fig. 19

Network impulse response:
double time series; N = 3.

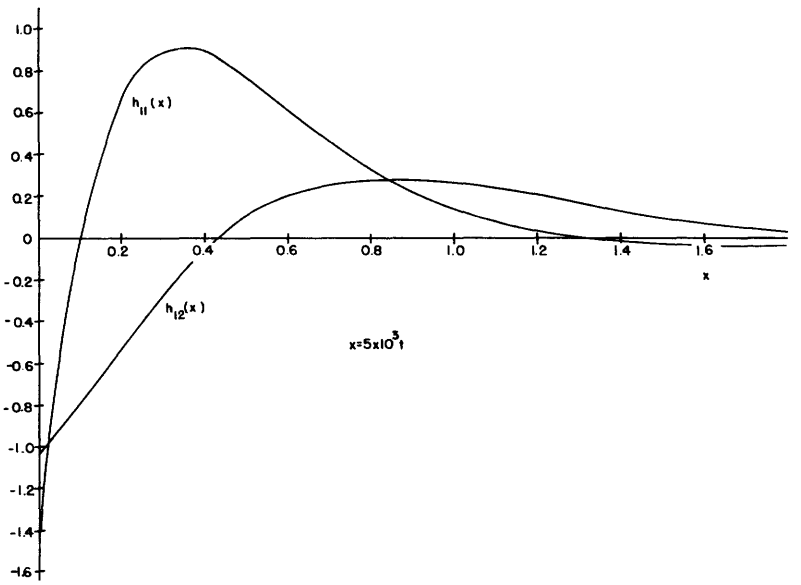

Fig. 20

Network impulse response:
double time series; N = 4.

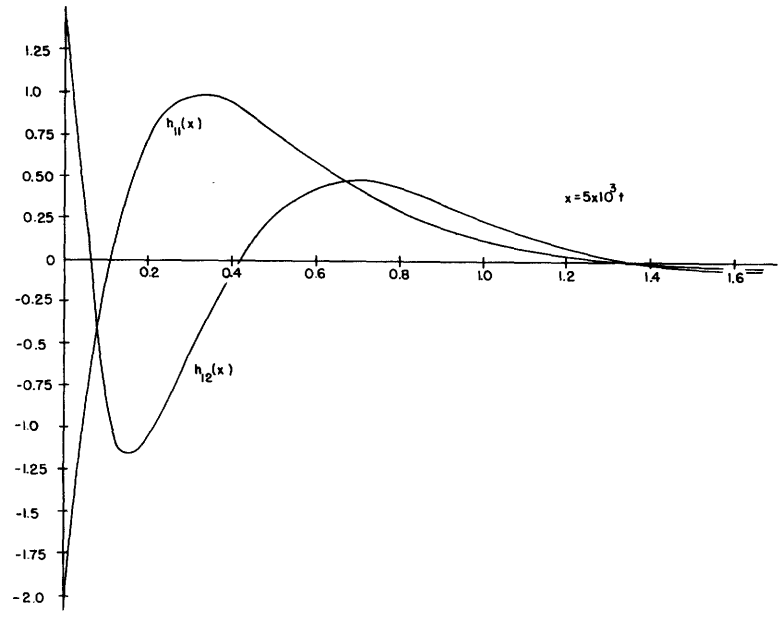

Fig. 21

Network impulse response:
double time series; N = 5.

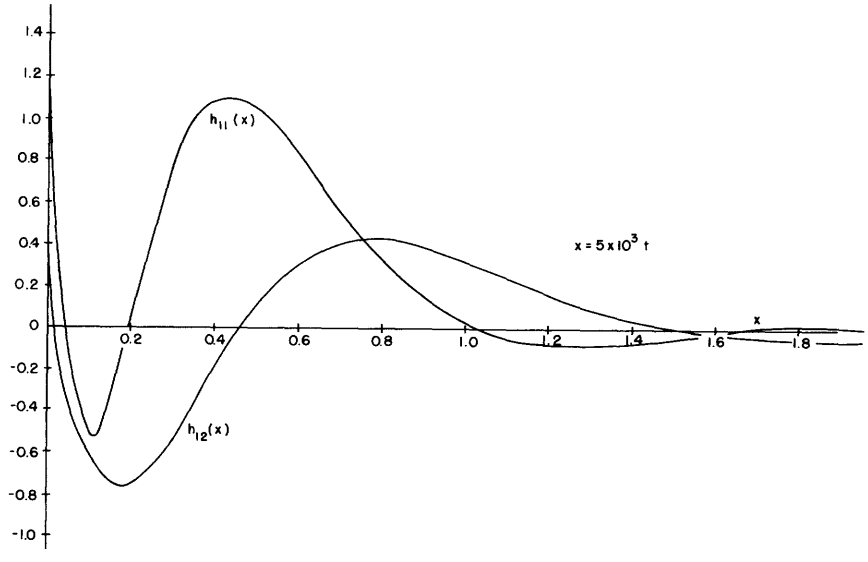

Fig. 22

Network impulse response:
double time series; N = 6.

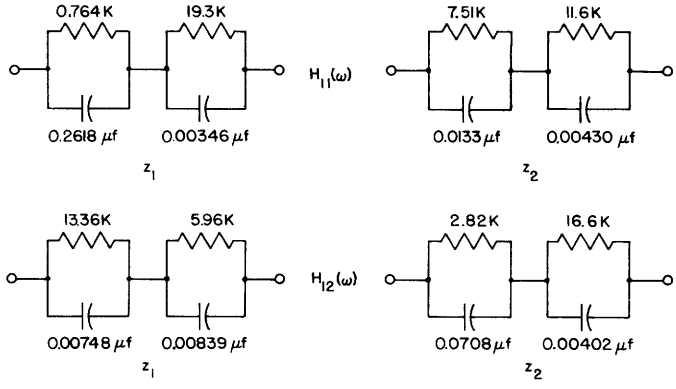

Fig. 23

Networks Z_1 and Z_2:
double time series; N = 4.

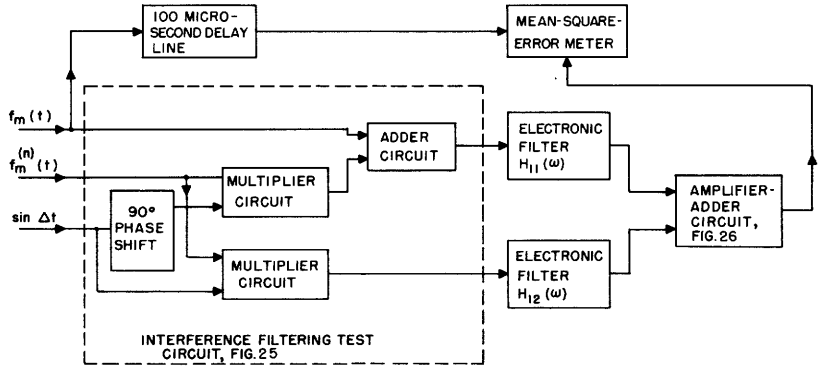

Fig. 24

Experimental test set-up:
double time series.

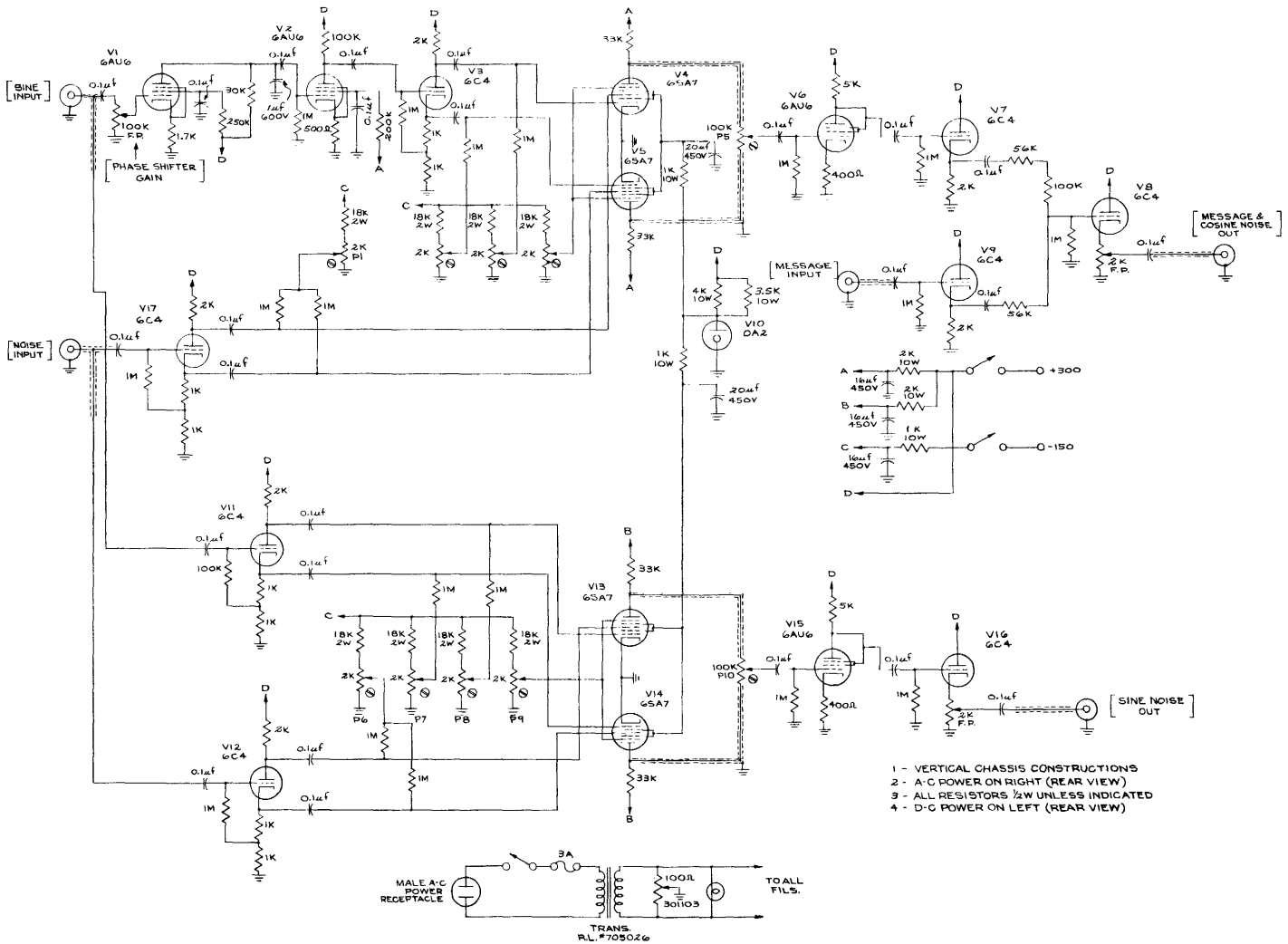

Fig. 25

Interference filtering test circuit.

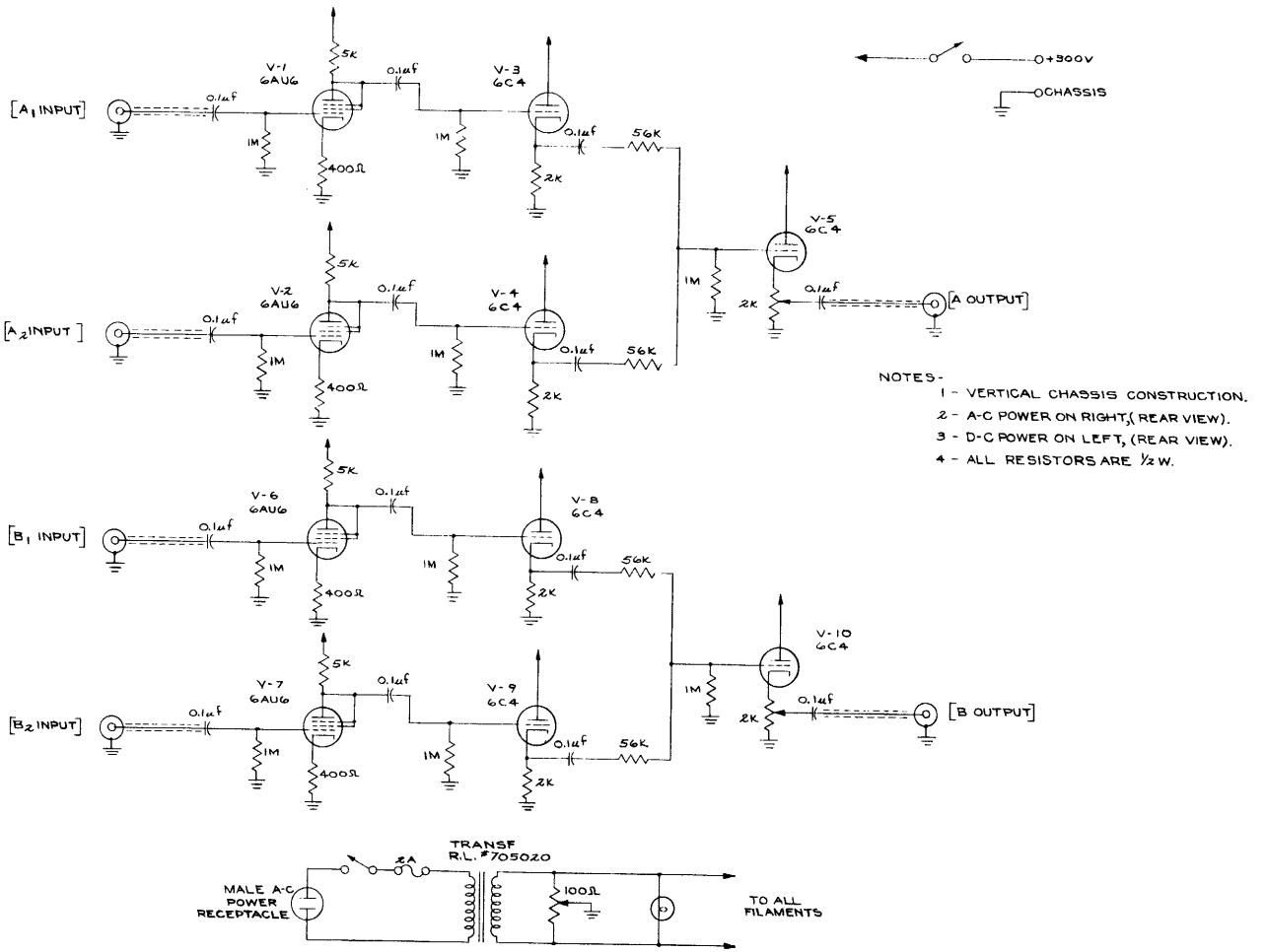

Fig. 26

Amplifier-adder circuit.

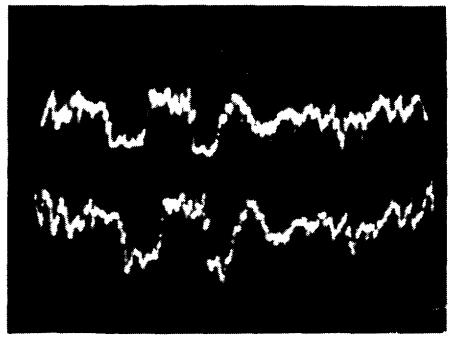

A– MESSAGE INPUT, $f_m(t)$
B– DELAY LINE OUTPUT

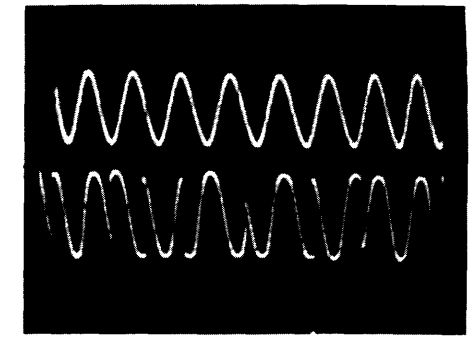

A– SINΔt INPUT
B– $H_{12}(\omega)$ INPUT

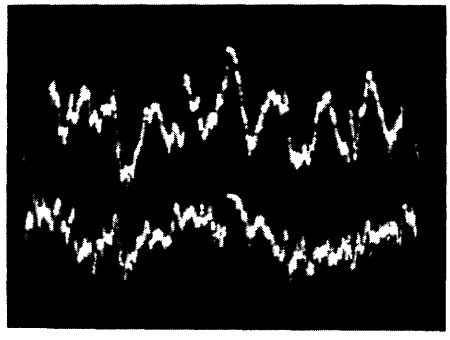

A– $H_{11}(\omega)$ INPUT
B– MESSAGE INPUT, $f_m(t)$

A– UPPER TRACE
B– LOWER TRACE

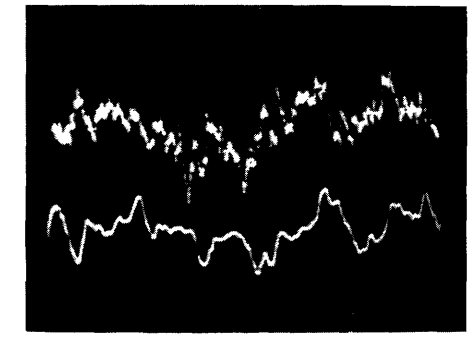

A– DELAY LINE OUTPUT
B– AMPLIFIER - ADDER OUTPUT

TRACE DESCRIPTIONS REFER TO FIGURE 24

Fig. 27
Experimental test set-up oscillographs.

VI. Conclusion

The statistical approach to filter design as originally conceived by Wiener and later developed by Lee is just beginning to come into general use. It seems appropriate to conclude this report by a brief discussion of the advantages to be gained by substituting statistical design methods for the conventional ones.

For the single time series filter one must not expect greatly improved performance to result from the new method. For example, it has been shown (ref. 20) that for certain message and noise situations a conventional Butterworth filter will give a mean-square error of output which is very nearly that obtainable by the optimum statistical filter. On the other hand the statistical methods of filter design are of an exact nature. Once the correlation functions of the message and noise are known the optimum filter characteristics may be determined. In this respect it is interesting to observe that the filter design work of Sec. V could have been done by someone quite unfamiliar with

filter design techniques. One could even build a machine which would compute filter parameters from given correlation data. It might be said that the design of filters is an art when using conventional methods and becomes an exact science when the statistical approach is employed.

When dealing with multiple time series the systematic approach of the statistical method becomes even more important. Design techniques for the treatment of several channel voltages by conventional methods are unavailable unless the cross-channel relationships are of a rather simple nature. For this reason it is believed that there may exist many practical problems involving multiple time series which may be treated much more satisfactorily by the methods of this report.

Table II

N	1	2	3	4	5	6
c_1^{11}	+0.56037	+0.31125	-1.22168	+0.38158	+0.29408	-0.92599
c_2^{11}		+0.44206	+7.57798	-7.51342	-5.03243	+29.0283
c_3^{11}			-6.53750	+28.9270	+14.6605	-237.498
c_4^{11}				-23.2832	+3.42800	+730.390
c_5^{11}					-15.4189	-899.337
c_6^{11}						+379.707
c_1^{12}	0	+0.74514	+0.33221	-1.41210	+2.86000	+1.65913
c_2^{12}		-1.03175	+1.21125	+13.3636	-41.9777	-35.3767
c_3^{12}			-2.51992	-24.8938	+185.355	+208.060
c_4^{12}				+11.9144	-290.923	-447.391
c_5^{12}					+146.067	+391.280
c_6^{12}						-117.929
ε_{min}	0.506	0.482	0.371	0.318	0.313	0.279

Acknowledgment

The author wishes to express his gratitude to Professors Norbert Wiener, R. M. Fano, and J. B. Wiesner for their many helpful comments and suggestions. The author is especially grateful to Professor Y. W. Lee for the time he has so generously given in supervising this research.

References

1. N. Wiener: Cybernetics, Wiley, 1948
2. N. Wiener: The Extrapolation, Interpolation, and Smoothing of Stationary Time Series with Engineering Applications, Wiley, 1949
3. C. E. Shannon, W. Weaver: The Mathematical Theory of Communication, University of Illinois Press, 1949
4. R. M. Fano: The Transmission of Information, Technical Report No. 65, Research Laboratory of Electronics, M.I.T. March 1949
5. R. M. Fano: The Transmission of Information-II, Technical Report No. 149, Research Laboratory of Electronics, M.I.T. Feb. 1950
6. Y. W. Lee: Course 6.563, Statistical Communication Theory, Class Notes, unpublished
7. N. Wiener: Generalized Harmonic Analysis, Acta Mathematica, 55, 1930
8. H. Cramer: Mathematical Methods of Statistics, Princeton University Press, 1946
9. G. Szego: Orthogonal Polynomials, 23, Am. Math. Soc. Colloquium Publications, 1939
10. D. Jackson: Fourier Series and Orthogonal Polynomials, Carus Mathematical Monograph No. 6, Math. Assoc. of America, 1941
11. E. A. Guillemin: Communication Networks-II, Wiley, 1935
12. E. A. Guillemin: RC-Coupling Networks, Report No. 43, Radiation Laboratory, M.I.T. Oct. 1944
13. E. A. Guillemin: Courses 6.561, 6.562, Advanced Network Theory, Class Notes, unpublished
14. N. Wiener and Y. W. Lee: U. S. Patents No. 2,128,257; 2,024,900; 2,124,599
15. E. A. Guillemin: Procedure for Synthesizing RC Networks, unpublished
16. D. G. Tucker: The Synchrodyne, Electronic Engineering, May, June, Sept. 1947
17. D. G. Tucker: A Two-Phase Telemetering System, Electronic Engineering, May, June 1948
18. D. B. Harris: Selective Demodulation, Proc. I.R.E. 35, 565, June 1947
19. C. A. Stutt: An Experimental Study of Optimum Filters, Technical Report No. 182, Research Laboratory of Electronics, M.I.T. May 1951
20. C. A. Stutt: An Experimental Study of Optimum Linear Systems, Doctoral thesis, Electrical Engineering, M.I.T. 1951
21. R. Talimberas: Master's thesis, Electrical Engineering, M.I.T. June 1950